Supporting Information for

Conformationally Locked BODIPY Donor–Acceptor Dyads: Charge Separation and Recombination across a [2.2.2]Bicyclooctane Spacer

Contents

1. General Procedures

^{1}H and ^{13}C NMR spectra were recorded on a Bruker Avance III 500 MHz spectrometer. Chemical shifts are reported as ppm relative to TMS and referenced to residual solvent peaks of CDCl3 (δ 7.26 ppm). Multiplicity assignments are abbreviated as follows: s = singlet, d = doublet, t = triplet, q = quartet, m = multiplet.

UV-Vis absorption spectra were recorded in solutions using Shimadzu UV-1900i and PerkinElmer Lambda 900 UV/VIS/NIR spectrometers (1 cm path length quartz cell). Fluorescence emission spectra were measured using FluoroMax-4 spectrometer. Emission quantum yields of the compounds were measured relative to the fluorescence of Rhodamine 6G as a standard (Φ_F = 0.95 in ethanol).[1] Sample concentrations were chosen to obtain an absorbance of 0.03-0.07 at the excitation wavelength; at least three measurements were performed for each sample.

Excited state lifetimes were determined by time-correlated single photon counting (TCSPC) measurements using Horiba Scientific DeltaHub DH-HT High throughput TCSPC module equipped with a DeltaDiode-510L pulsed laser diode with peak wavelength 510nm +/-10nm. Datastation v2.4 software was used for data collection and analysis was conducted on Eztime software. Decay curves were fitted with mono- and bi-exponential functions and the quality was determined by the $\chi 2$ values.

The UV-Vis absorption spectra of radical anions and cations were recorded using an Agilent 8453 UV-visible spectrophotometer. Luminescence lifetime measurements were carried out on an OB920 spectrometer (Edinburgh Instruments, UK) using time-correlated single photon counting (TCSPC). All samples were degassed by bubbling argon for approximately 15 minutes prior to measurement.

Transient absorption spectra were acquired using an apparatus based on a Ti:sapphire regenerative amplifier (Coherent Legend Elite), providing 40 fs pulses centred at 800 nm, with an average power of 3.2 W and 1 kHz repetition rate. The system was pumped by a commercial Ti:sapphire oscillator (Coherent Micra). The output of the amplifier was split to generate the pump and probe pulses. Pump pulses at 490 nm were produced by mixing the signal output of a commercial optical parametric amplifier (TOPAS, Light Commercial) with the 800 nm fundamental output in a BBO crystal. The probe and reference pulses were obtained by focusing a small portion of the laser output on a 3 mm thick CaF_2 plate. The polarization angle between the pump and probe beam was set to the magic angle by rotating a $\lambda/2$ plate. The measurements were performed in a quartz cell (2 mm optical path length), mounted on a movable stage to avoid photodegradation and multiple excitations of the sample. The data were analyzed with a global fitting procedure using the GLOTARAN package and applying a linear sequential model. (*J. Stat. Softw.,* **2012**, *49*, 1-22.)

Nanosecond transient absorption (ns-TA) measurements were performed using an LP980 laser flash photolysis spectrometer (Edinburgh Instruments, UK). Transient signals were digitized with a Tektronix TDS 3012B oscilloscope, and the kinetic traces and difference absorption spectra were analyzed using L900 software. All samples were deaerated by purging with nitrogen for approximately 15 minutes prior to measurement. Excitation was provided by a tunable nanosecond pulsed laser (Opolette™ 355II+UV, OPOTEK, USA; wavelength range: 210–2400 nm), operated at a typical pulse energy of 5 mJ.

Mass spectrometry analysis (HRMS) was performed with a Q-Tof Premier Waters MALDI quadrupole time-of-flight (Q-TOF) mass spectrometer equipped with Z-spray electrospray ionization (ESI) and matrix assisted laser desorption ionization (MALDI) sources in positive mode with *trans*-2-[3-(4-tertbutylphenyl)-2-methyl-2-propenylidene]malononitrile as the matrix. ESI mass spectra were acquired in positive modes as required, using a Micromass TOF mass spectrometer interfaced to a Waters 2960 HPLC or a Bruker microTOF-Q III spectrometer interfaced to a Dionex UltiMate 3000 LC. Atmospheric pressure chemical ionization (APCI) experiments were performed on a Bruker microTOF-Q III spectrometer interfaced to a Dionex UltiMate 3000 LC.

2. Synthetic Procedures and Characterization

The handling of all air/water sensitive materials was carried out using standard high vacuum techniques. Tetrahydrofuran and dichloromethane were distilled from $LiAlH_4$ and CaH_2, respectively. All other solvents were used as commercially supplied. Analytical thin layer chromatography was performed using silica gel 60 (fluorescence indicator F254, pre-coated sheets, 0.2 mm thick, 20 cm × 20 cm; Merck) plates and visualized by UV irradiation (λ = 254 nm). Column chromatography was carried out using Kieselgel Gel 60 (0.063-0.2 mm).

1,8-Diazabicyclo[5.4.0]undec-7-ene, Oxone® monopersulfate compound, ethyl isocyanoacetate, 2,4-dimethyl-1-*H*-pyrrole, boron trifluoride diethyl etherate, *N*,*N*-diisopropylethylamine, ethyl 2,4-dimethyl-1*H*-pyrrole-3-carboxylate, phosphorus(V) oxychloride, potassium acetate and dimethylformamide were purchased from Sigma-Aldrich. Compound **PA-1** was prepared according to previously published procedures.[2]

Procedure for synthesis of pyrroles PA-2 and PA-3

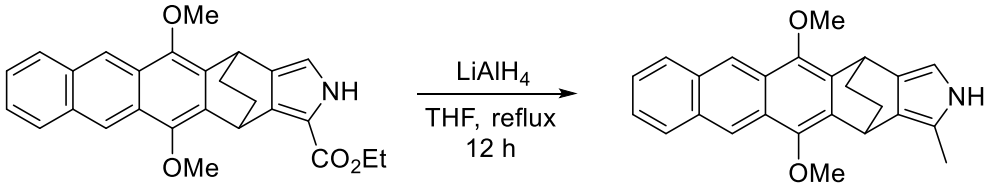

The compound **PA-2** was prepared using a previously reported procedure.[3] $LiAlH_4$ (1 g, 26.3 mmol) was added to dry THF (50 mL) under nitrogen. The mixture was stirred and cooled to 0°C. **PA-1** (2 g, 4.67 mmol) was dissolved in dry THF (15 mL) and the solution was added dropwise into the reaction flask. The mixture was heated under reflux for 12 h, cooled to room temperature and subsequently to 0°C. An aqueous solution of NaOH (10%, 10 mL)) was added slowly to quench the residual $LiAlH_4$. The resulting mixture was filtered through a short layer of silica (5 cm) which was then washed with THF (30 mL). The solvent was removed *in vacuo* to give the target compound, **PA-2** (1 g, 58% yield).

PA-2 (1 g, 58% yield). ^{1}H NMR (400 MHz, $CDCl_3$) δ 8.60 (s, 2H), 8.03 (dd, 2H), 7.45 (dd, 2H), 7.39 (s, 1H), 6.51 (d, *J* = 4.1 Hz, 1H), 4.79 (d, *J* = 9.4 Hz, 2H), 4.05 (d, *J* = 1.4 Hz, 2H), 2.32 (s, 2H), 1.35 – 1.22 ppm (m, 3H). ^{13}C NMR (101 MHz, $CDCl_3$) δ 145.11, 144.91, 133.42, 133.26, 131.32, 130.21, 129.22, 128.50, 128.49, 127.61, 126.78, 126.74, 125.23, 123.52, 120.85, 120.79, 118.63, 106.96, 62.62, 31.17, 29.98, 27.88, 22.80, 11.35 ppm.

General procedure for synthesis of FPA-1 and FPA-2

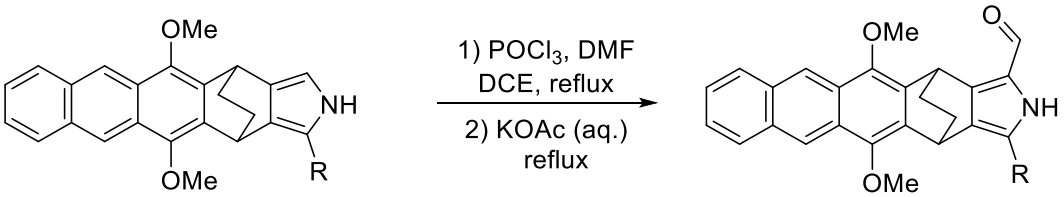

PA-1, PA-2 **FPA-1, FPA-2**

Compounds **FPA-1** and **FPA-2** were prepared using a modified literature procedure.[4]

FPA-1: Phosphorous(V) oxychloride (0.789 g, 5.15 mmol,) was added to DMF (0.376 g, 5.15 mmol) at 5°C under N_2 and the resulting mixture was left to stir for 10 mins. The mixture was then diluted with 10 mL of 1,2-dichloroethane (DCE) A solution of **PA-1** (2 g, 4.68 mmol) was in DCE (30 mL) was then added dropwise over 1 hour at 10°C. The reaction mixture was left to stir at room temperature for 1

hour, followed by heating at reflux under N_2 for another hour. The rection mixture was subsequently cooled to room temperature, followed by addition of potassium acetate (2.30 g, 23.4 mmol) in H_2O (20 mL). The reaction mixture was then heated at reflux under N_2 for an additional 20 mins. The crude product was extracted with DCM (2 × 50 mL). The combined organic extracts were dried over Na_2SO_4 and concentrated *in vacuo*. The crude product was purified by recrystallizing from MeOH at -20 °C over 72 hours, followed by further chromatographic purification. This was done using DCM-packed silica, with neat DCM as the eluent, later switching to a 30:1 eluent system of DCM-ethyl acetate, yielding. **FPA-1.**

FPA-2: Synthesized from **PA-2** following a similar procedure to **FPA-1** with modifications. The amount of starting material was decreased to 1 g (3 mmol) and the amounts of all reagents were scaled down proportionately. Recrystallization was done from MeOH-Acetone (10:1), and no further chromatographic purification was required, yielding **FPA-2**.

FPA-1 (84%, 1.98 g).^{1}H NMR (400 MHz, $CDCl_3$) δ 9.93 (s, 1H), 9.29 (s, 1H), 8.62 (d, *J* = 8.3 Hz, 2H), 8.03 (dd, 2H), 7.51 – 7.41 (m, 2H), 5.40 (s, 1H), 5.25 (s, 1H), 4.53 – 4.36 (m, 2H), 4.06 (d, *J* = 6.7 Hz, 6H), 2.01 – 1.81 (m, 4H), 1.47 ppm (t, *J* = 7.1 Hz, 3H). ^{13}C NMR (101 MHz, $CDCl_3$) δ 178.39, 160.90, 146.03, 145.93, 139.08, 135.21, 131.64, 131.62, 130.56, 130.19, 128.54, 126.78, 126.55, 126.21, 125.71, 121.29, 121.18, 120.41, 63.02, 62.93, 61.40, 31.03, 30.26, 27.03, 26.66, 14.59 ppm.

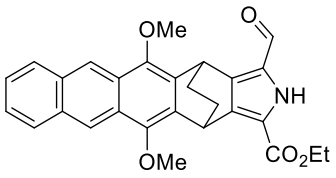

FPA-1

FPA-2 (1 g, 93%). ^{1}H NMR (400 MHz, $CDCl_3$) δ 9.64 (s, 1H), 9.06 (s, 1H), 8.60 (d, *J* = 3.1 Hz, 2H), 8.02 (dd, *J* = 6.5, 3.3 Hz, 2H), 7.53 – 7.41 (m, 2H), 5.17 (s, 1H), 4.81 (d, *J* = 2.5 Hz, 1H), 4.04 (s, 6H), 2.38 (s, 3H), 1.99 – 1.78 ppm (m, 4H). ^{13}C NMR (101 MHz, $CDCl_3$) δ 175.26, 145.90, 145.22, 141.34, 131.98, 131.57, 131.50, 130.75, 129.73, 128.54, 128.48, 128.06, 126.64, 126.57, 125.60, 125.56, 124.05, 121.15, 121.04, 62.83, 62.79, 30.59, 29.87, 27.52, 27.02, 11.69 ppm.

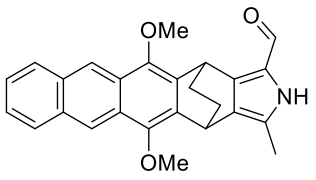

FPA-2

General procedure for the synthesis of compounds DMA-BDP 1-4 and BDP 1-2

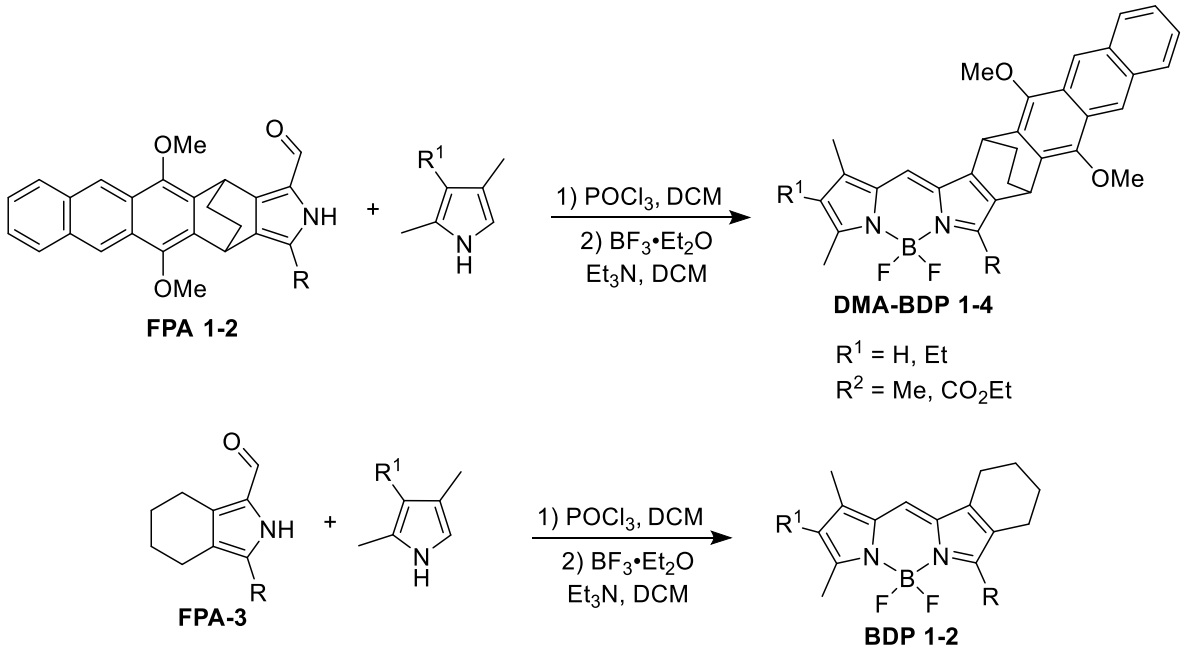

Compounds **DMA-BDP 1-4 and BDP 1-2** were prepared using a modified literature procedure.[5] A mixture of formylpyrrole (**FPA 1-3**, 1 mmol) and corresponding pyrrole (1 mmol) in 20-40 mL of dichloromethane (DCM) was cooled with an ice bath under flow of N_2. Phosphorus(V) oxychloride (0.184 g, 1.2 mmol) was then added in one portion. The reaction mixture was left to stir for 16 h at room temperature. After stirring, the reaction was cooled with an ice bath and Et_3N (0.506 g, 5 mmol), followed by $BF_3.Et_2O$ (0.852 g, 6 mmol) was then added dropwise, and the resulting mixture was left to stir for an additional 2 hr at room temperature. The mixture was then diluted with DCM (50 mL), washed with H_2O (2 × 50 mL), dried over Na_2SO_4 and evaporated in vacuum. The resulting crude compound was then purified chromatographically, using hexane – packed silica, with hexane – ethyl acetate (4:1) as the eluent.

DMA-BDP-1 (49% yield). ^{1}H NMR (400 MHz, $CDCl_3$) δ 8.60 (d, *J* = 7.9 Hz, 2H), 8.12 – 7.94 (m, 2H), 7.64 – 7.40 (m, 2H), 6.05 (s, 1H), 5.01 (s, 1H), 4.84 (s, 1H), 4.05 (d, *J* = 0.5 Hz, 6H), 2.64 (s, 3H), 2.53 (s, 3H), 2.29 (s, 3H), 1.98 – 1.78 ppm (m, 4H). ^{13}C NMR (101 MHz, $CDCl_3$) δ 158.16, 148.54, 147.83, 145.87, 145.41, 142.11, 135.94, 134.32, 131.62, 131.54, 131.52, 130.29, 128.55, 128.50, 127.65, 126.67, 126.46, 125.65, 125.63, 121.20, 121.07, 120.22, 119.60, 62.91, 31.64, 30.51, 27.36, 27.18, 14.93, 12.87, 11.59 ppm. UV-vis (CH_2Cl_2): λ_{max} [nm] (log ε) = 520 (4.86). HRMS (APCI): *m/z* found 394.167446, calcd for (M+) $C_{22}H_{21}BF_2N_2O_2$ 394.1664.

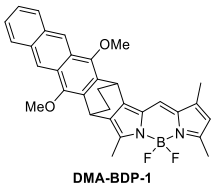

DMA-BDP-1

DMA-BDP-2 (50% yield) ^{1}H NMR (400 MHz, $CDCl_3$) δ 8.60 (d, *J* = 8.7 Hz, 2H), 8.06 – 7.99 (m, *J* = 8.9, 3.2 Hz, 2H), 7.49 – 7.43 (m, 2H), 7.15 (s, 1H), 4.99 (s, 1H), 4.82 (s, 1H), 4.05 (d, *J* = 1.5 Hz, 5H), 2.62 (s, 3H), 2.51 (s, 3H), 2.38 (q, *J* = 7.6 Hz, 2H), 2.22 (s, 3H), 1.95 – 1.80 (m, 5H), 1.07 ppm (t, *J* = 7.6 Hz, 3H). ^{13}C NMR (101 MHz, $CDCl_3$) δ 158.03, 146.75, 146.63, 145.78, 145.34, 138.33, 135.00, 133.99, 133.03, 131.76, 131.60, 131.52, 130.55, 128.55, 128.50, 127.03, 126.69, 126.47, 125.60, 125.59, 121.18, 121.03, 119.33, 62.89, 31.67, 30.48, 27.39, 27.24, 17.44, 14.57, 12.97, 12.76, 9.65 ppm. UV-vis (CH_2Cl_2): λ_{max} [nm] (log ε) = 531 (4.89). HRMS (APCI): *m/z* found 573.249267, calcd for (M+Na) $C_{34}H_{33}BF_2N_2NaO_2$ 573.250130.

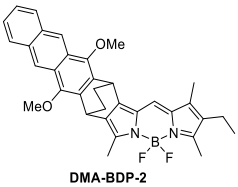

DMA-BDP-2

DMA-BDP-3 (12% yield) ^{1}H NMR (400 MHz, $CDCl_3$) δ 8.61 (d, *J* = 20.4 Hz, 2H), 8.06 – 7.98 (m, 2H), 7.52 – 7.43 (m, 2H), 7.35 (s, 1H), 6.25 (s, 1H), 5.45 (t, *J* = 2.4 Hz, 1H), 5.02 (t, *J* = 2.4 Hz, 1H), 4.50 (q, *J* = 7.1 Hz, 2H), 4.06 (d, *J* = 5.2 Hz, 6H), 2.65 (s, 3H), 2.36 (s, 2H), 1.96 – 1.79 (m, 5H), 1.54 ppm (t, *J* = 7.1 Hz, 4H). ^{13}C NMR (101 MHz, $CDCl_3$) δ 168.13, 160.77, 146.80, 145.82, 145.47, 143.64, 138.74, 131.46, 131.41, 131.00, 130.30, 128.46, 128.32, 127.98, 127.96, 126.69, 126.32, 125.49, 125.47, 123.65, 121.59, 121.22, 120.81, 62.94, 62.76, 60.93, 32.01, 31.02, 27.27, 26.51, 15.83, 14.43, 11.56 ppm. UV-vis (CH_2Cl_2): λ_{max} [nm] (log ε) = 507 (4.63). HRMS (APCI): *m/z* found 603.2247, calcd for (M+Na) $C_{34}H_{31}BF_2N_2NaO_2$ 603.2243.

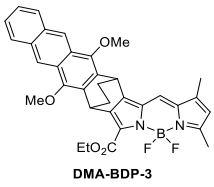

DMA-BDP-3

DMA-BDP-4 (34% yield) ^{1}H NMR (400 MHz, $CDCl_3$) δ 8.61 (d, *J* = 20.8 Hz, 2H), 8.06 – 7.99 (m, 2H), 7.50 – 7.43 (m, 2H), 5.45 (s, 1H), 5.00 (s, 1H), 4.49 (q, 2H), 4.06 (d, *J* = 7.6 Hz, 6H), 2.63 (s, 3H), 2.42 (q, *J* = 7.6 Hz, 2H), 2.26 (s, 3H), 2.05 (s, 1H), 1.54 (t, *J* = 7.1 Hz, 3H), 1.09 ppm (t, *J* = 7.6 Hz, 3H).^{13}C NMR (101 MHz, $CDCl_3$) δ 168.61, 160.85, 145.77, 145.39, 142.28, 141.14, 138.46, 137.23, 131.44, 131.39, 131.15, 130.52, 129.88, 128.45, 128.31, 127.76, 126.70, 126.33, 125.45, 125.43, 121.19, 120.77, 120.05, 62.93, 62.72, 60.77, 32.03, 30.92, 27.29, 26.51,

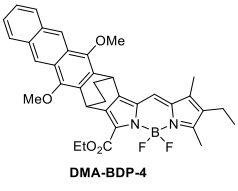

DMA-BDP-4

17.38, 14.45, 14.20, 13.95, 9.54 ppm. UV-vis (CH_2Cl_2): λ_{max} [nm] (log ε) = 493 (4.46). HRMS (APCI): *m/z* found 631.256433, calcd for (M+Na) $C_{36}H_{35}BF_2N_2NaO_2$ 631.255642.

BDP-1 (82% yield) ^{1}H NMR (400 MHz, $CDCl_3$) δ 6.92 (s, 1H), 5.98 (s, 1H), 2.62 (s, 2H), 2.49 (d, *J* = 17.5 Hz, 6H), 2.37 (s, 1H), 2.21 (s, 3H), 1.82 – 1.73 ppm (m, 4H). ^{13}C NMR (101 MHz, $CDCl_3$) δ 156.19, 154.63, 141.11, 139.56, 132.56, 132.20, 128.98, 119.06, 118.09, 77.48, 77.16, 76.84, 23.03, 22.55, 21.55, 21.02, 14.78, 14.64, 12.73, 11.39, 11.33 ppm. UV-vis (CH_2Cl_2): λ_{max} [nm] (log ε) = 519 (4.77). HRMS (APCI): *m/z* found 311.150974, calcd for (M+Na) $C_{16}H_{19}BF_2N_2NaO_2$ 311.150450.

BDP-1

BDP-2 (22% yield)^{1}H NMR (400 MHz, $cdcl_3$) δ 6.88 (s, 1H), 2.62 (s, 2H), 2.47 (d, *J* = 15.2 Hz, 7H), 2.38 (q, *J* = 7.6 Hz, 5H), 2.15 (s, 3H), 1.81 – 1.71 (m, 4H), 1.06 ppm (t, *J* = 7.6 Hz, 4H). ^{13}C NMR (101 MHz, $CDCl_3$) δ 154.42, 154.15, 140.11, 136.43, 132.16, 131.55, 128.14, 118.42, 77.48, 77.16, 76.84, 29.84, 23.13, 22.66, 21.57, 21.05, 17.42, 14.74, 12.62, 9.51 ppm. UV-vis (CH_2Cl_2): λ_{max} [nm] (log ε) = 532 (4.34). HRMS (APCI): *m/z* found 339.182073, calcd for (M+Na) $C_{18}H_{23}BF_2N_2NaO_2$ 339.181785.

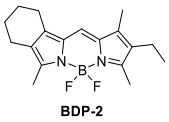

BDP-2

3. NMR Spectra

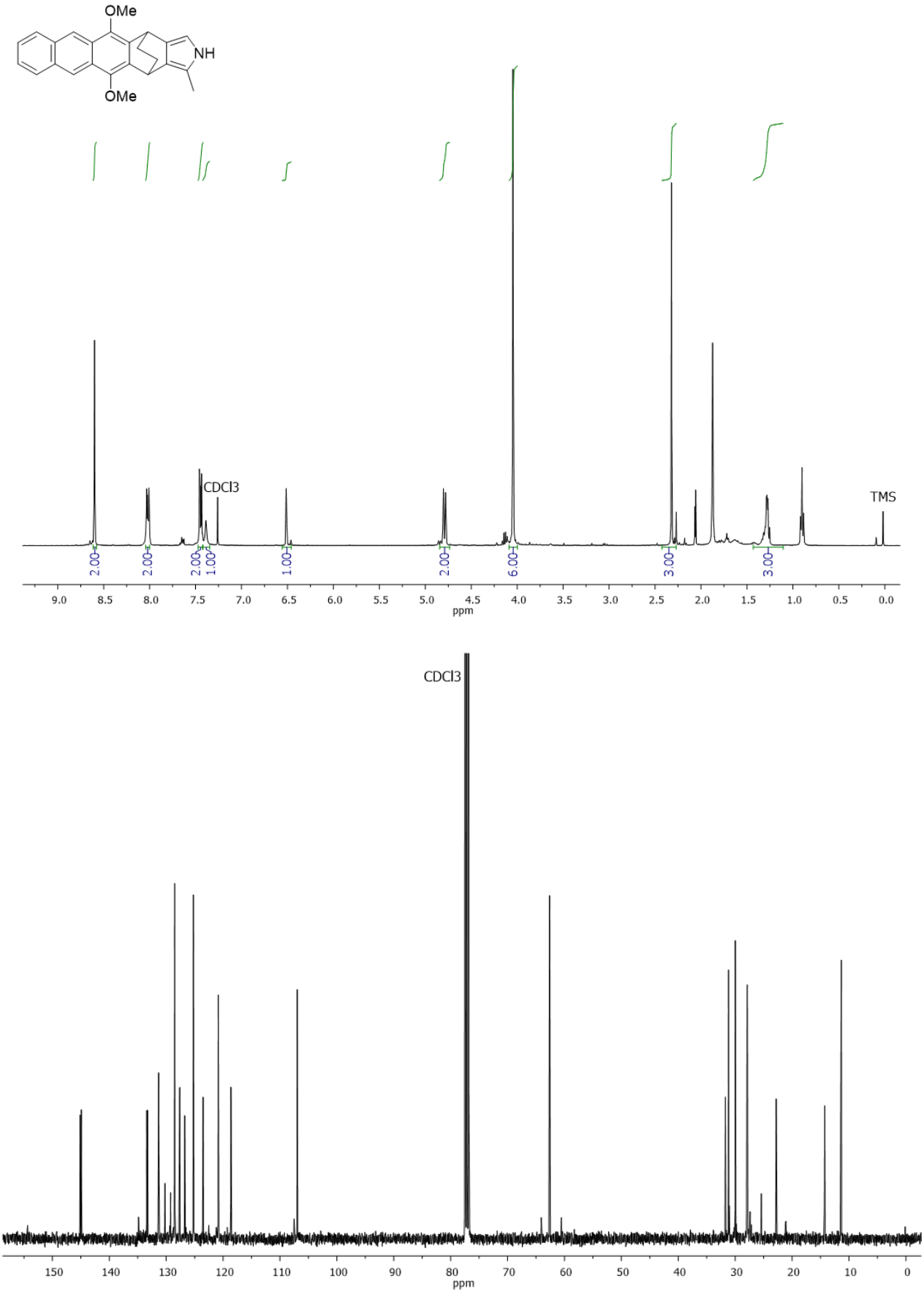

Figure S1. ^{1}H and ^{13}C NMR spectra of compound **PA-2**.

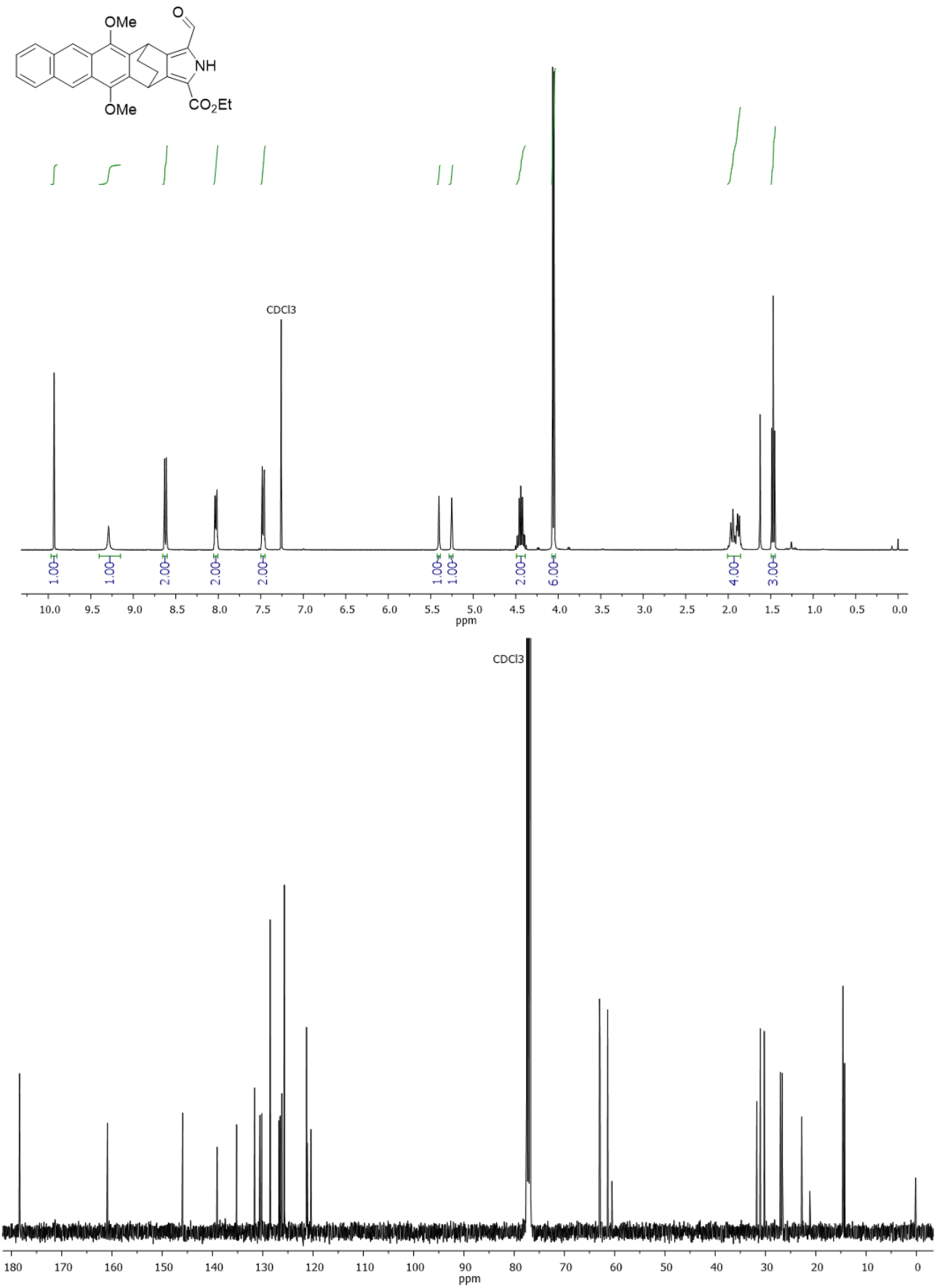

Figure S2. ^{1}H (400 MHz) and ^{13}C (101 MHz) NMR spectra of compound **FPA-1** in $CDCl_3$.

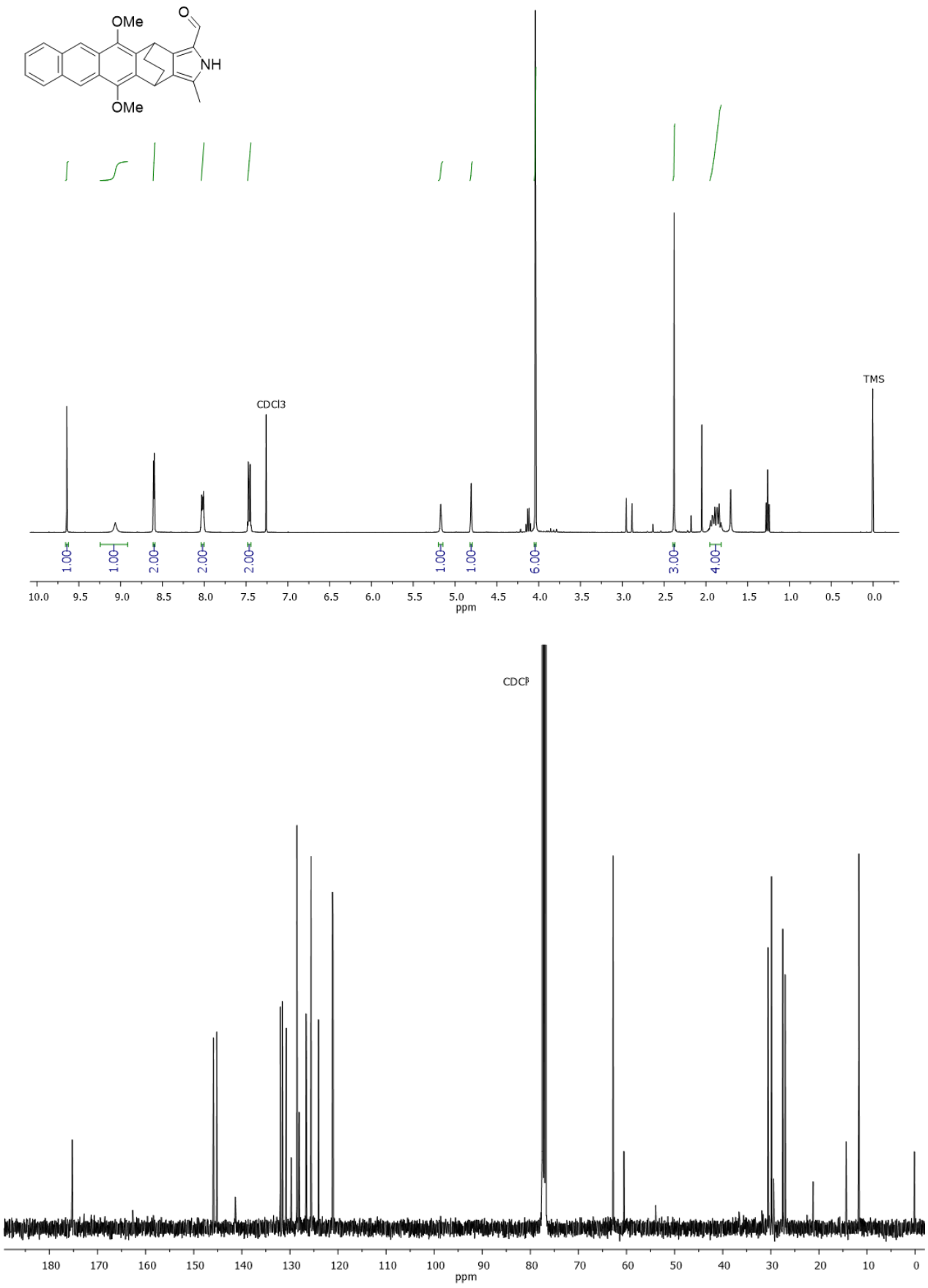

Figure S3. ^{1}H (400 MHz) and ^{13}C (101 MHz) NMR spectra of compound **FPA-2** in $CDCl_3$.

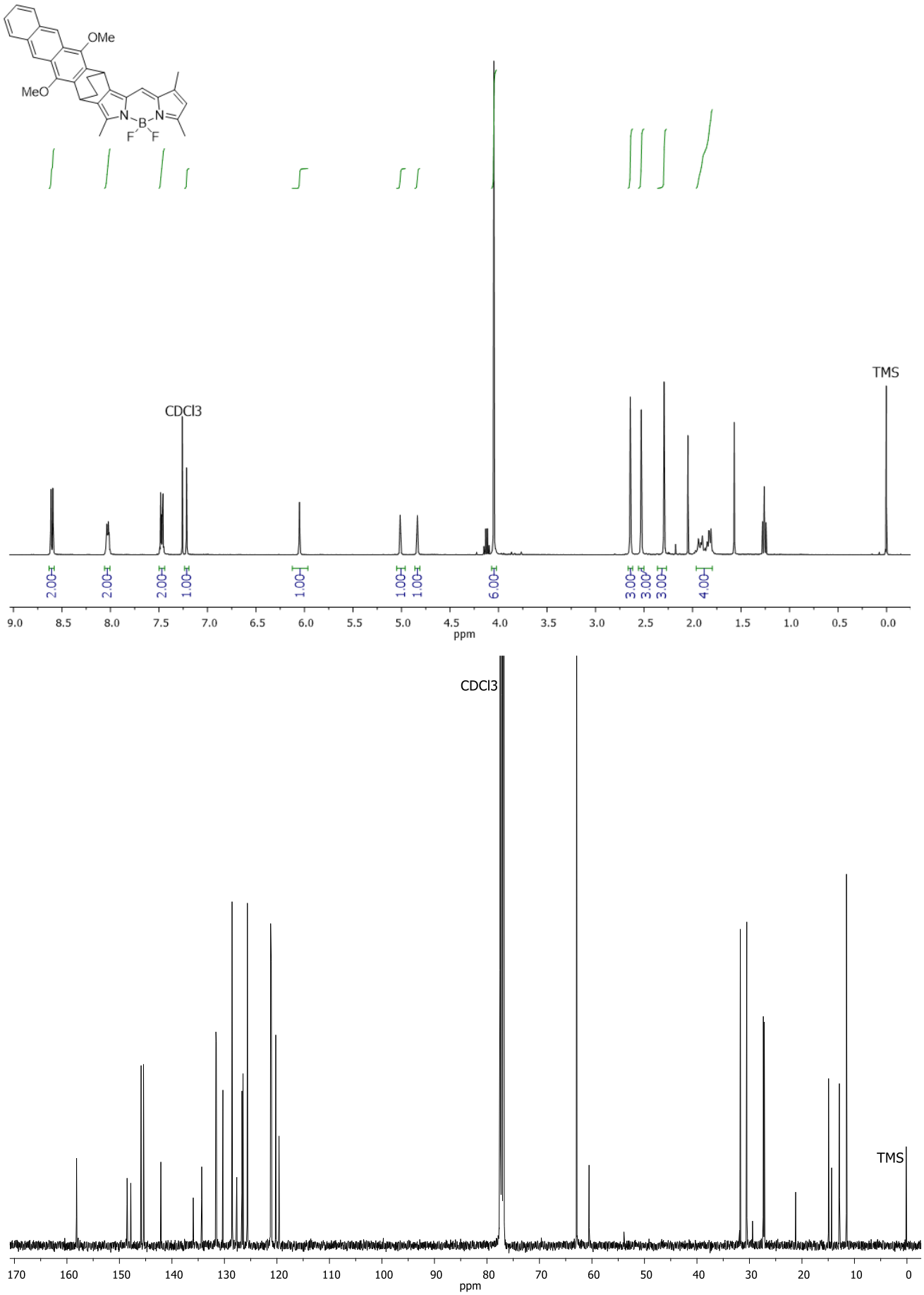

Figure S4. ^{1}H (400 MHz) and ^{13}C (101 MHz) NMR spectra of compound **DMA-BDP-1** in $CDCl_3$.

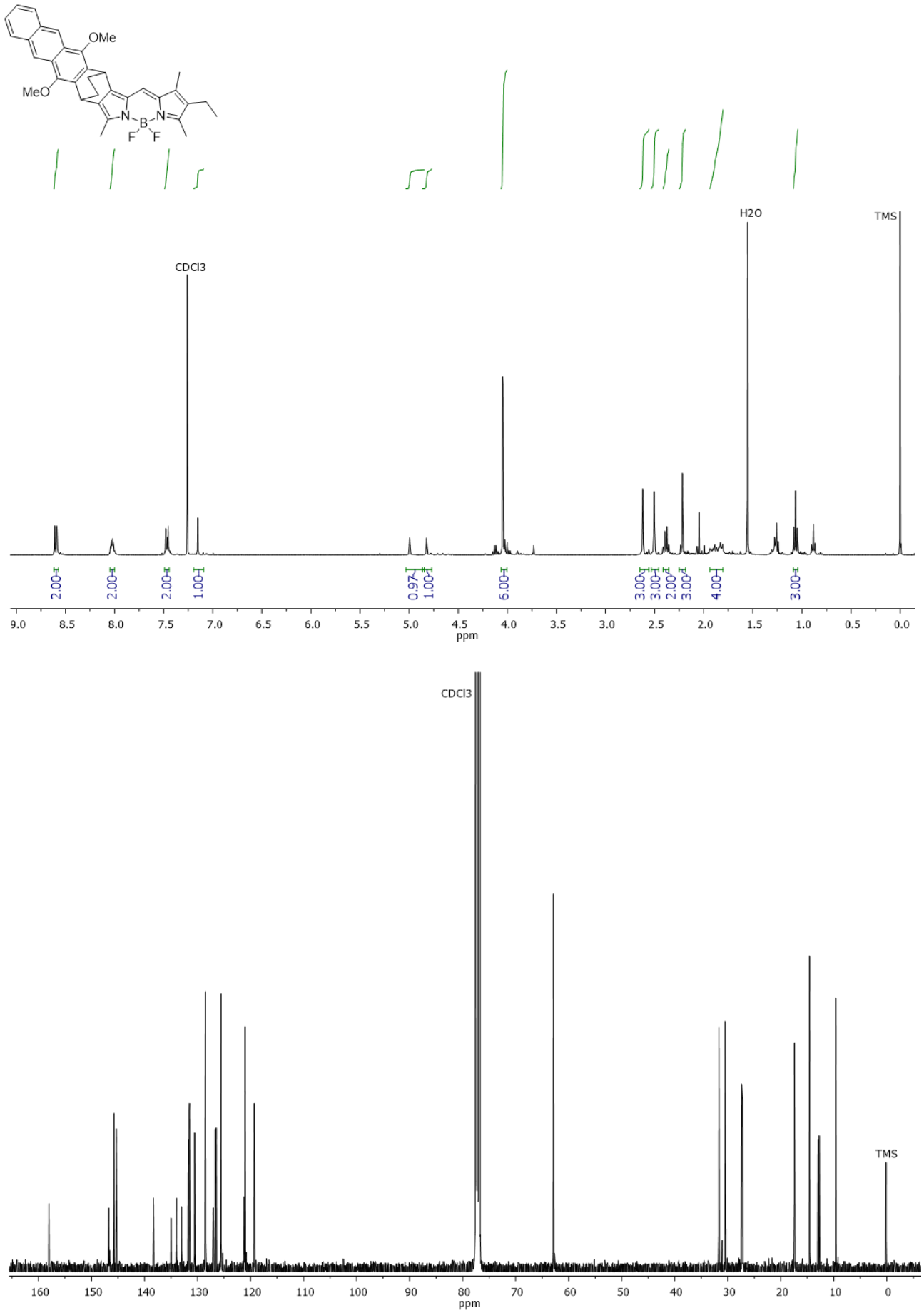

Figure S5. ^{1}H (400 MHz) and ^{13}C (101 MHz) NMR spectra of compound **DMA-BDP-2** in $CDCl_3$.

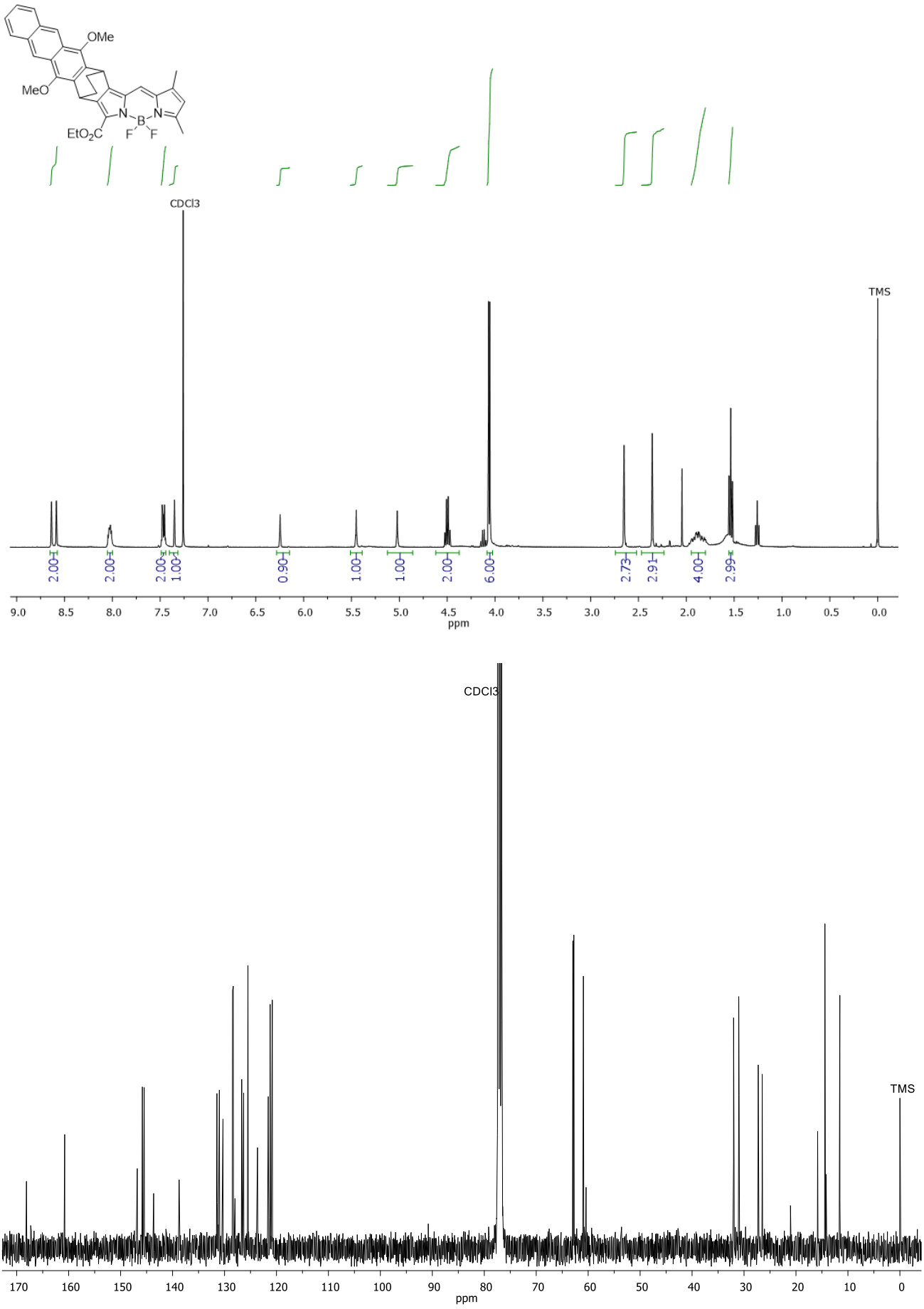

Figure S6. ^{1}H (400 MHz) and ^{13}C (101 MHz) NMR spectra of compound **DMA-BDP-3** in $CDCl_3$.

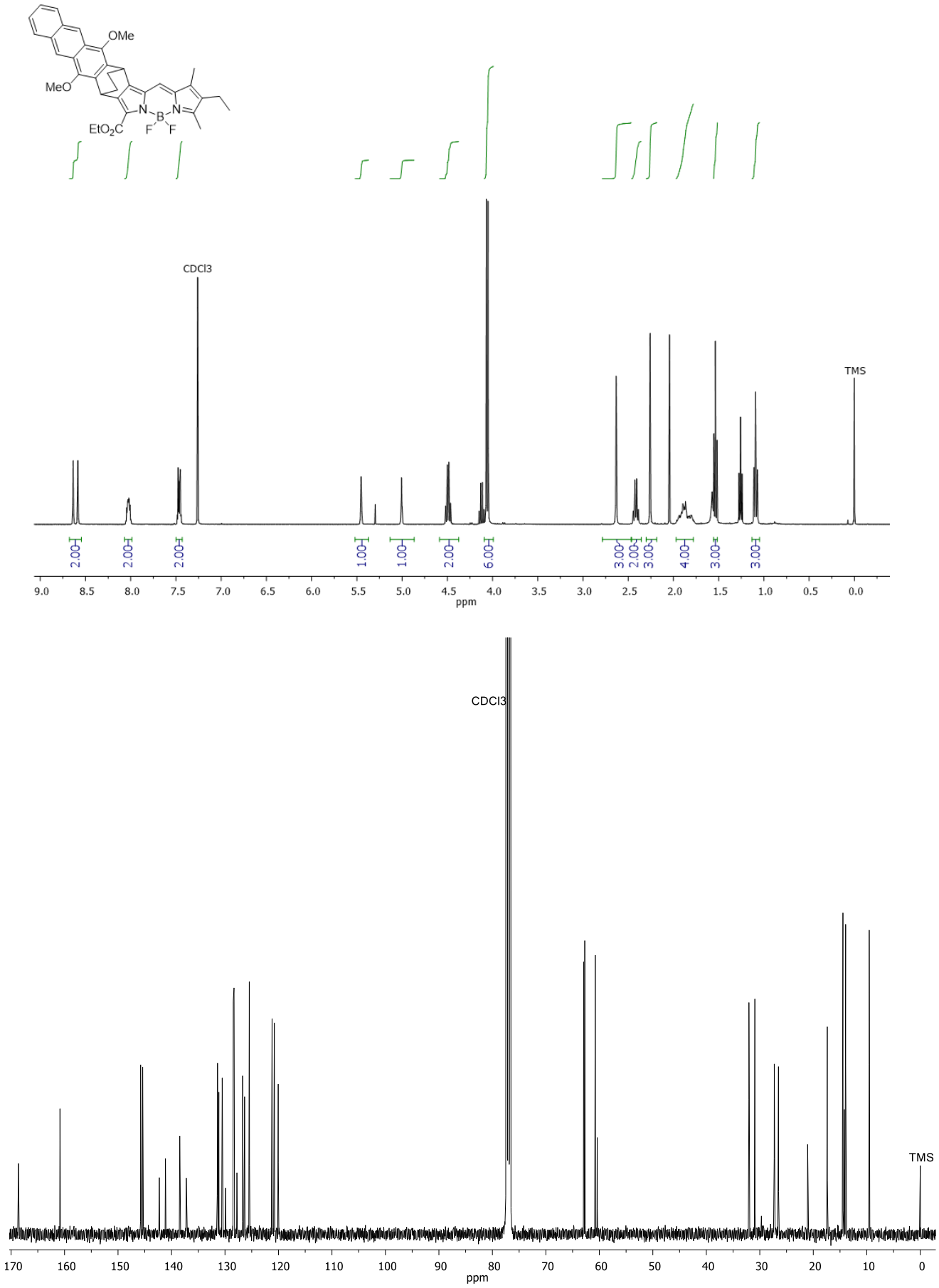

Figure S7. ^{1}H (400 MHz) and ^{13}C (101 MHz) NMR spectra of compound **DMA-BDP-4** in $CDCl_3$.

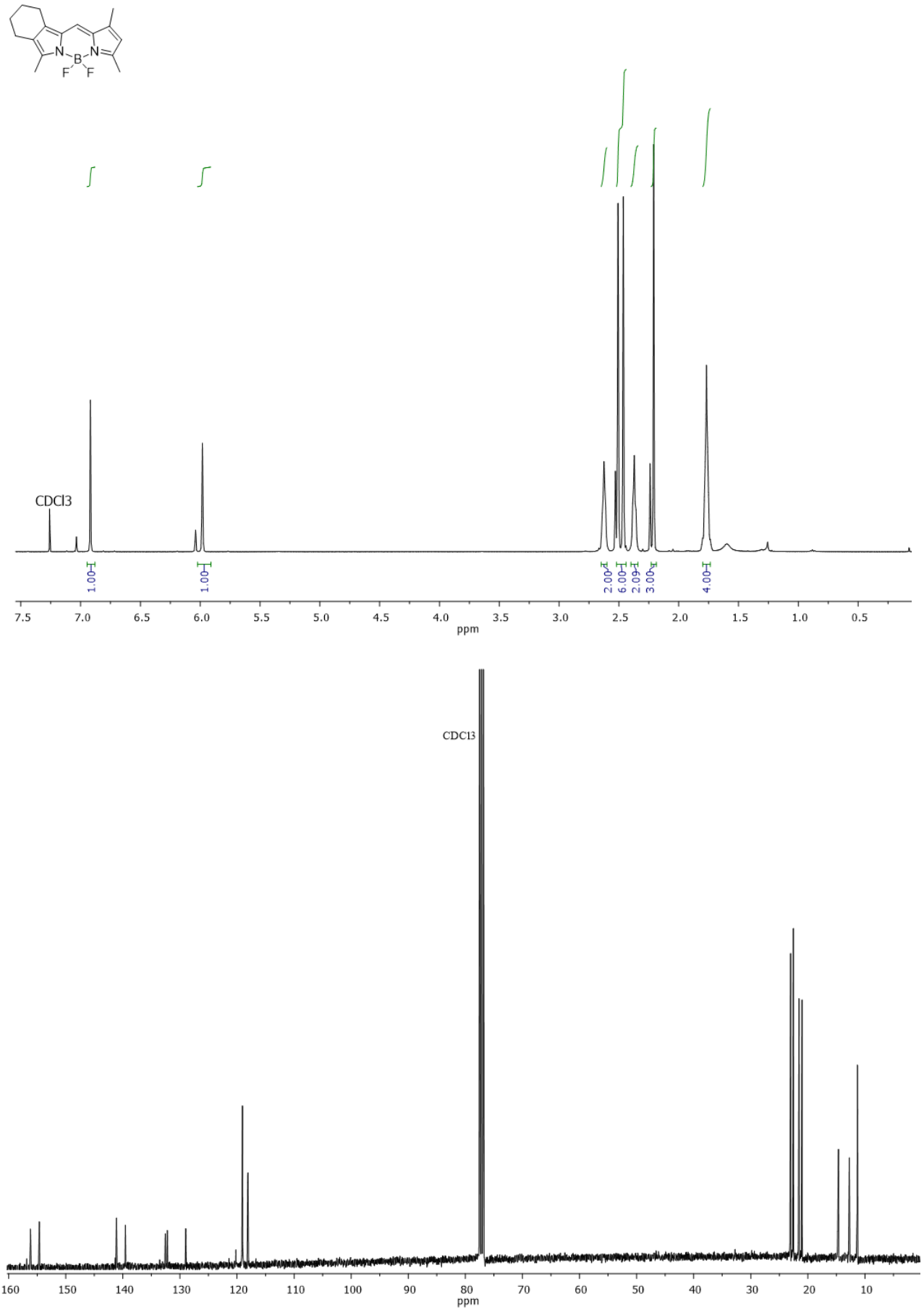

Figure S8. ^{1}H (400 MHz) and ^{13}C (101 MHz) NMR spectra of compound **BDP-1** in $CDCl_3$.

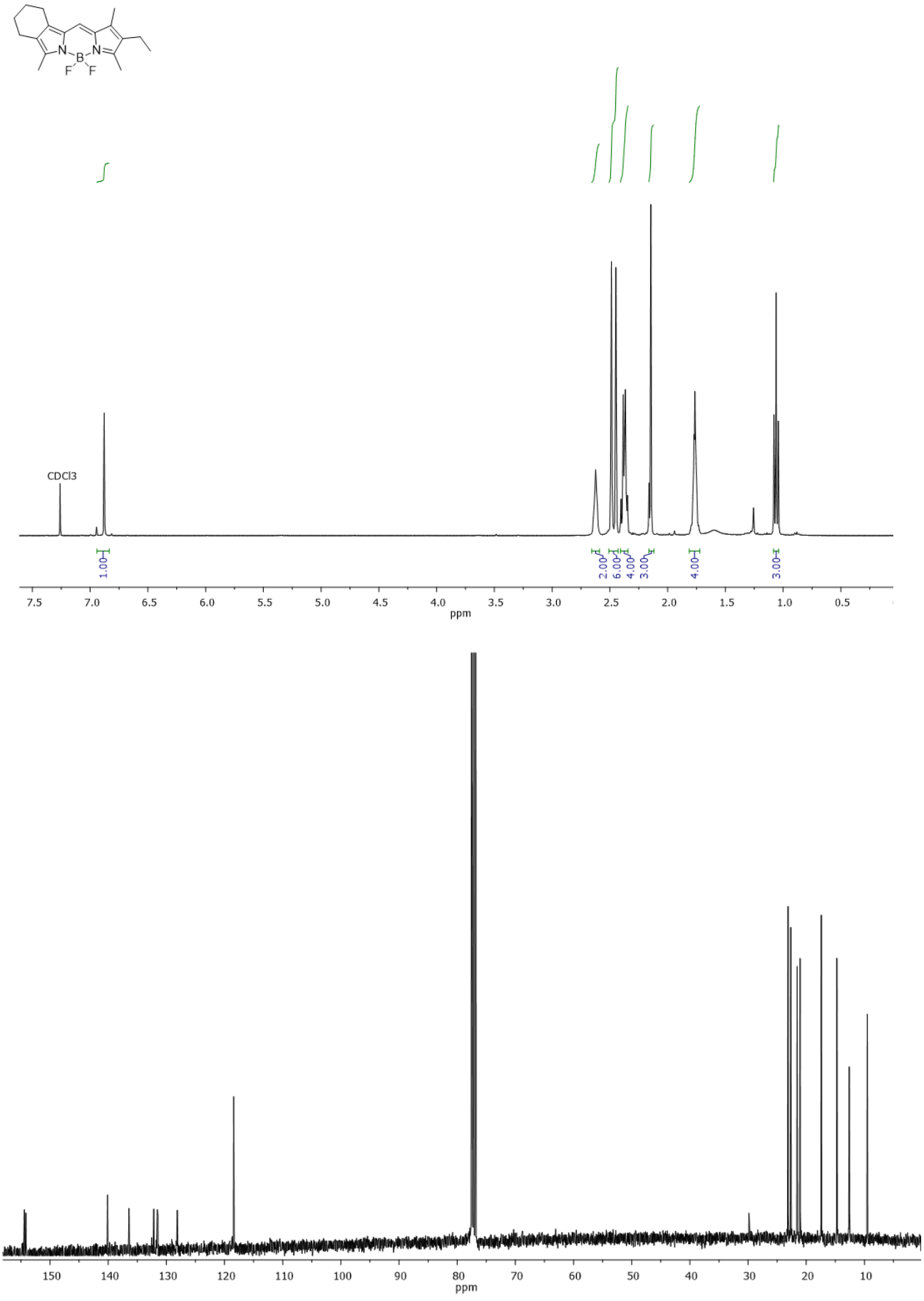

Figure S9. ^{1}H (400 MHz) and ^{13}C (101 MHz) NMR spectra of compound **BDP-2** in $CDCl_3$.

4. Optical Properties

4.1 Steady state optical properties of DMA-BDP-3 and DMA-BDP-4

Table S1. Optical properties of **DMA-BDP-3** and **DMA-BDP-4** in acetonitrile (ACN), ethyl acetate (EtOAc), dichloromethane (DCM), toluene (TOL) and cyclohexane (CYH).

Compound	Solvent[a]	λ_{abs} (nm)	λ_{em} (nm) [b]	$\Delta\lambda$ (nm)	Φ_{Fl}[c]
DMA-BDP-3	ACN	496	525	29	<0.01
	EtOAc	504	525	21	<0.01
	DCM	507	525	18	0.05
	TOL	515	531	16	0.02
	CYH	519	531	12	0.03
DMA-BDP-4	ACN	486	540	54	<0.01
	EtOAc	500	540	40	0.01
	DCM	493	540	47	<0.01
	TOL	523	543	20	<0.01
	CYH	528	540	12	0.23

4.2 Absorption and emission spectra of reference molecules

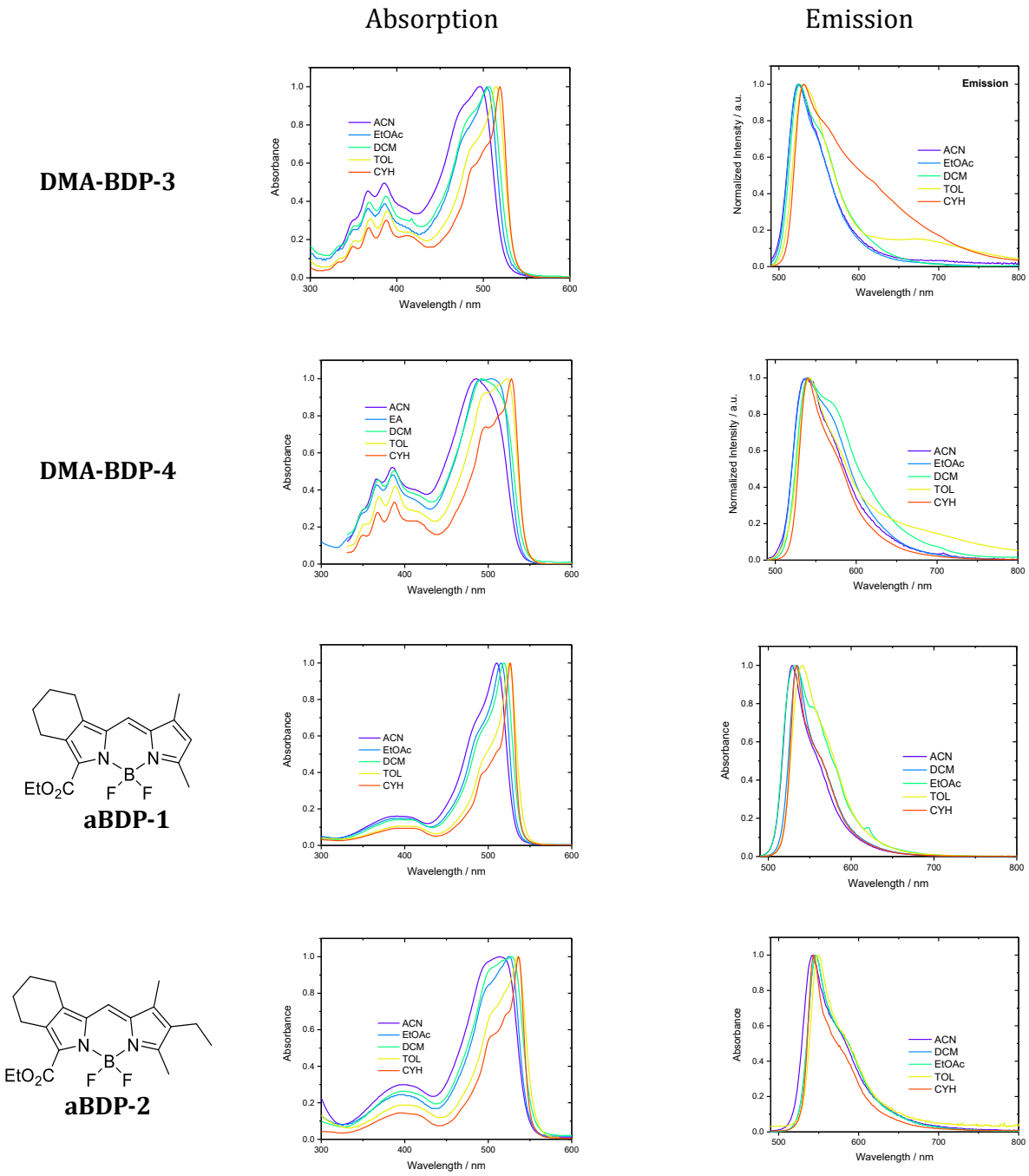

Figure S10. Normalized absorption and emission spectra of compounds **DMA-BDP3**, **DMA-BDP-4** and refence compounds **aBDP-1** and **aBDP-2** in different solvents: acetonitrile (ACN), ethyl acetate (EtOAc), dichloromethane (DCM), toluene (TOL), cyclohexane (CYH).

4.3 Overlaid absorption spectra of BDPs 1-2 with DMA

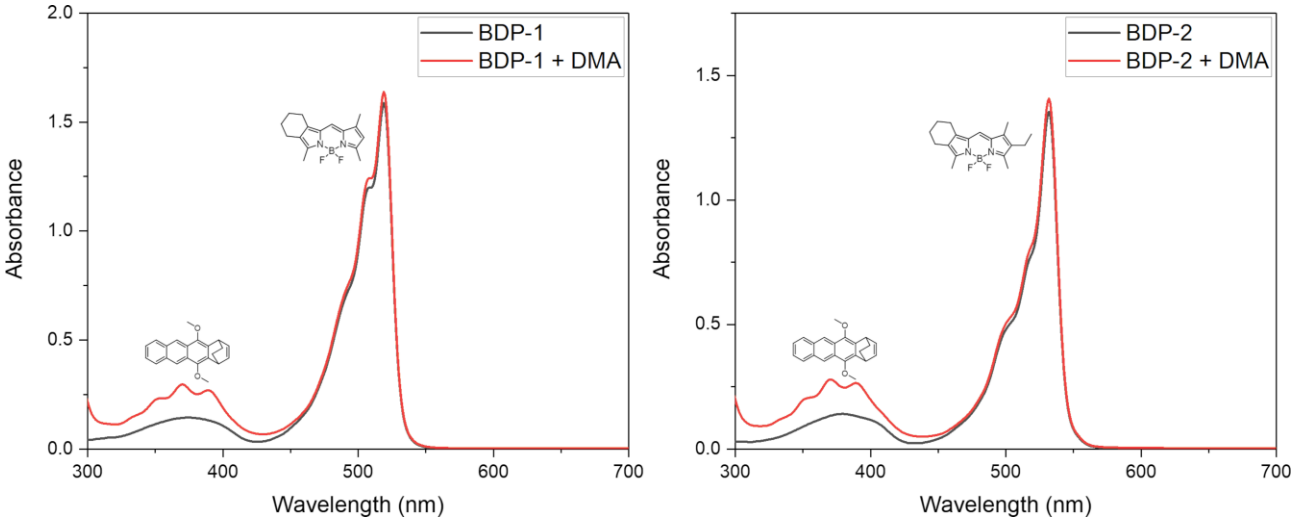

Figure S11. Overlay of the absorption spectra of the BDP reference compounds and spectra obtained after addition of DMA, in dichloromethane. (a) **BDP-1** and **BDP-1** with added DMA. (b) **BDP-2** and **BDP-2** with added DMA. The concentration of DMA was adjusted such that the relative optical densities of the DMA absorption band and the BDP absorption maximum reproduce those observed for the corresponding dyads (**DMA-BDP-1** and **DMA-BDP-2**). The resulting spectra show a clear increase in absorbance at 350 nm due to the contribution of the DMA chromophore.

4.4 Electrochemical measurements

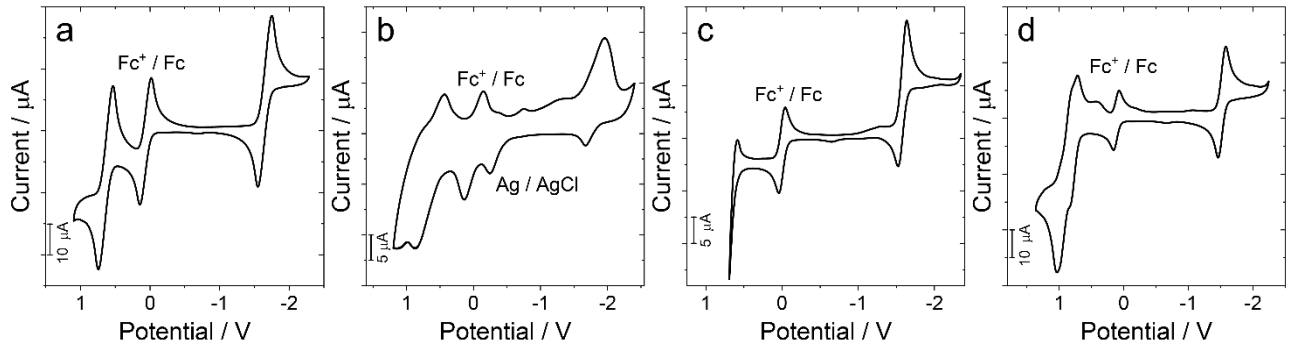

Figure S12. Cyclic voltammogram of the compounds. (a) **BDP-1**, (b) **BDP-2**, (c) **DMA-BDP-1** and (d) **DMA-BDP-2**. Ferrocene (Fc) was used as an internal reference. Measurements were carried out in degassed dichloromethane containing 0.10 M Bu_4NPF_6 as the supporting electrolyte, using a glassy carbon working electrode, platinum counter electrode, and $Ag/AgNO_3$ reference electrode. Scan rate: 100 mV/s. Concentration: 1.0×10^{-3} M. Temperature: 20 °C.

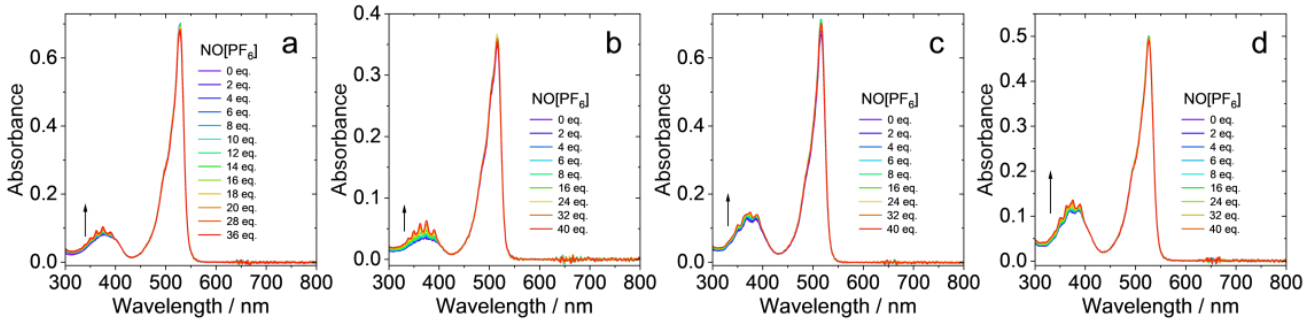

Figure S13. Evolution of the UV-Vis absorption spectra of (a) **BDP-1**, (b) **BDP-2**, (c) **DMA-BDP-1**, and (d) **DMA-BDP-2** upon addition of nitrosyl hexafluorophosphate ($NO[PF_6]$) as an oxidant in deaerated DMF. Conditions: c = 1.0 × 10^{-5} M, T = 20 °C.

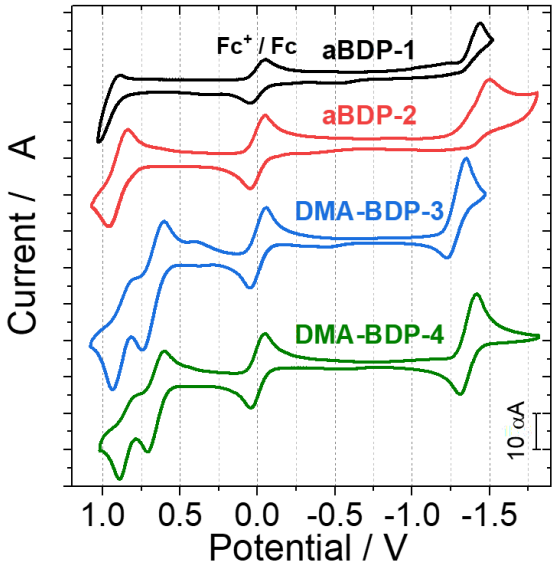

Figure S14**.** Cyclic voltammograms of **DMA-BDP-3**, **DMA-BDP-4** and the reference compounds **aBDP-1** and **aBDP-2**. Condition: in deaerated DCM containing 0.10 M $Bu_4[NPF_6]$ as the supporting electrode, $Ag/AgNO_3$ as the reference electrode. Scan rates: 100 mV/s. c = 1.0 × 10^{-3} M, 20 °C.

4.5 Gibbs Free Energy Changes of the Charge Separation and the Charge Transfer State Energy

The corresponding values were calculated using the Rehm-Weller equation:[6]

$$\Delta G_s = -\frac{e^2}{4\pi\varepsilon_s\varepsilon_0 R_{CC}} - \frac{e^2}{8\pi\varepsilon_0}\left(\frac{1}{R_D} + \frac{1}{R_A}\right)\left(\frac{1}{\varepsilon_{REF}} - \frac{1}{\varepsilon_s}\right) \quad (S1.)$$

$$\Delta G_{cs} = e(E_{OX} - E_{RED}) - E_{00} + \Delta G_s \quad (S2.)$$

$$E_{cs} = e(E_{OX} - E_{RED}) + \Delta G_s \quad (S3.)$$

The static Coulombic energy (ΔG_S) was calculated using the Rehm-Weller equation, where e represents the electronic charge, E_{OX} and E_{RED} are the half-wave potential of electron-acceptor unit for one electron reduction and one electron reduction, respectively, and E_{00} represents the singlet excited state energy (approximated from the crossing point of normalized UV-Vis absorption and fluorescence spectra). The solvent static dielectric constant (ε_S) and the dielectric constant of the electrochemical measurement solvent (ε_{REF}) were included, along with the vacuum permittivity (ε_0). R_{CC} stands for center-to-center distance between the electron donor unit and electron acceptor unit, determined by DFT optimization of the geometry, R_D, is the radius of the electron donor, R_A, is the radius of the electron acceptor. Calculations were performed for electron transfer in the following solvents: hexane (HEX, ε_S = 1.88), toluene (TOL, ε_S = 2.38), tetrahydrofuran (THF, ε_S = 7.6), dichloromethane (DCM, ε_S = 8.93), and acetonitrile (ACN, ε_S = 35.9).

4.6 Femtosecond Time-Resolved Transient Absorption Spectra

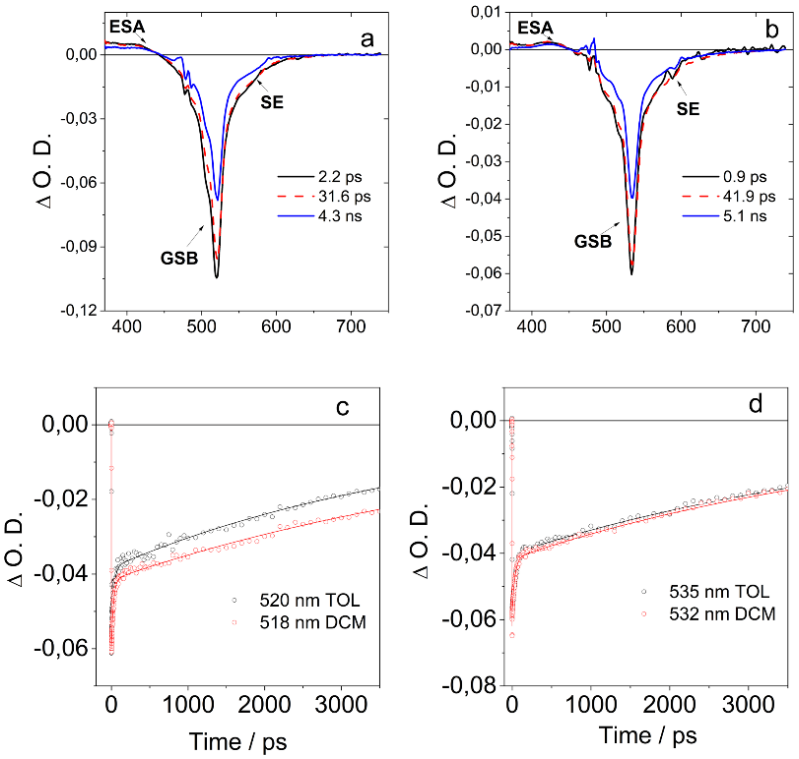

Figure S15. EADS obtained from global analysis of the transient data recorded for a) **BDP-1** and b) **BDP-2** in toluene. Panel c) and d) report the comparison of the kinetic traces measured for **BDP-1** (c) and **BDP-2** (d) in TOL and DCM.

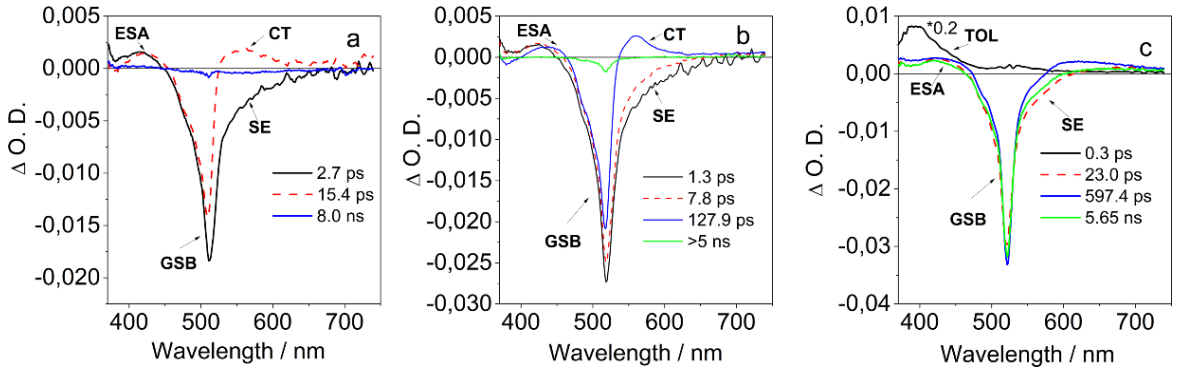

Figure S16. EADS obtained from global analysis of the transient data recorded for **DMA-BDP-1** in (a) ACN, (b) DCM and (c) toluene upon excitation at 350 nm.

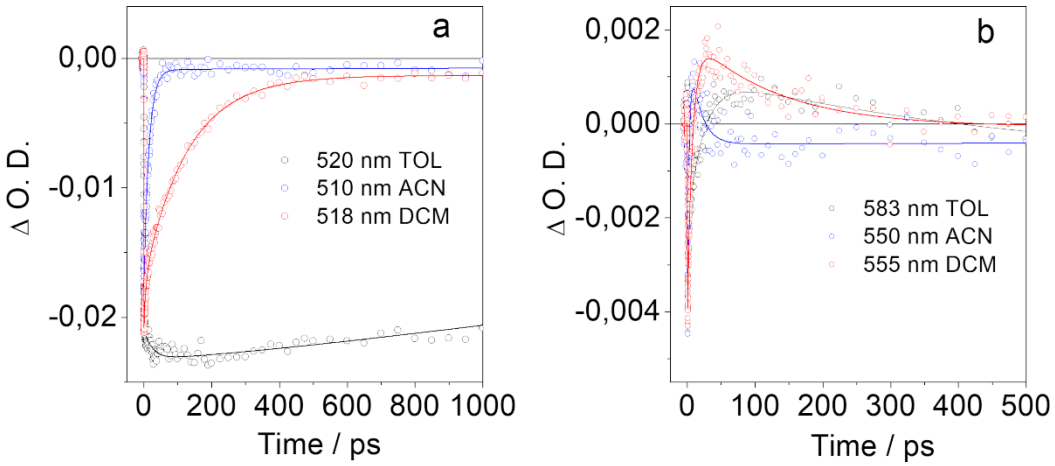

Figure S17. Selected kinetic traces recorded for **DMA-BDP1** in different solvents upon excitation at 350 nm.

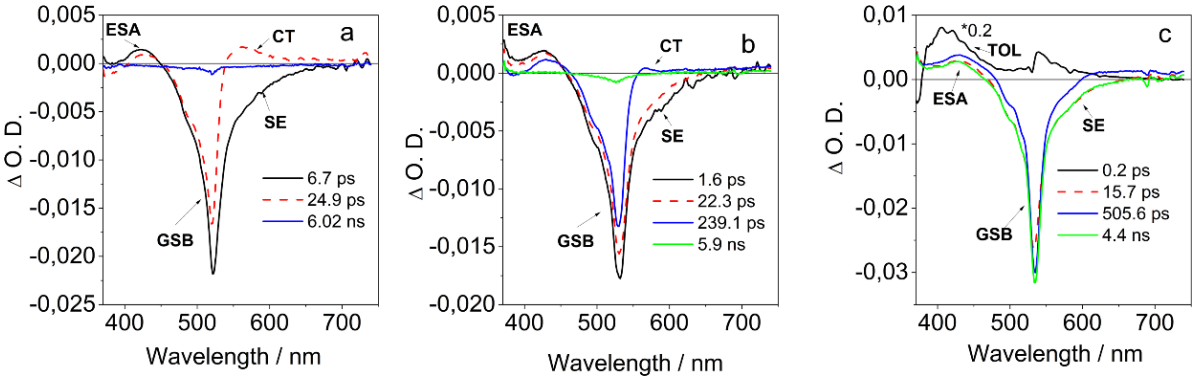

Figure S18. EADS obtained from global analysis of the transient data recorded for **DMA-BDP-2** in (a) ACN, (b) DCM and (c) toluene upon excitation at 350 nm.

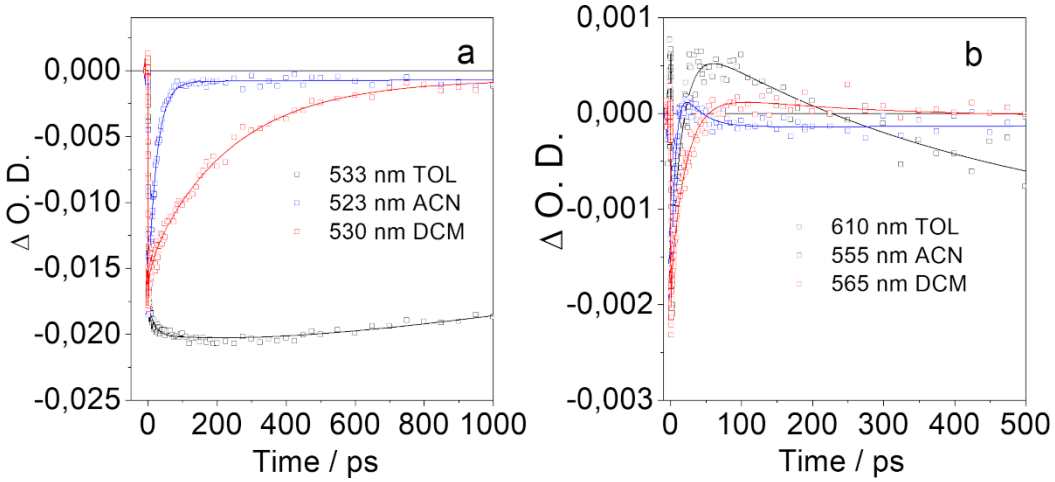

Figure S19. Selected kinetic traces recorded for **DMA-BDP-2** in different solvents upon excitation at 350 nm.

4.7 Nanosecond Time-Resolved Transient Absorption Spectra

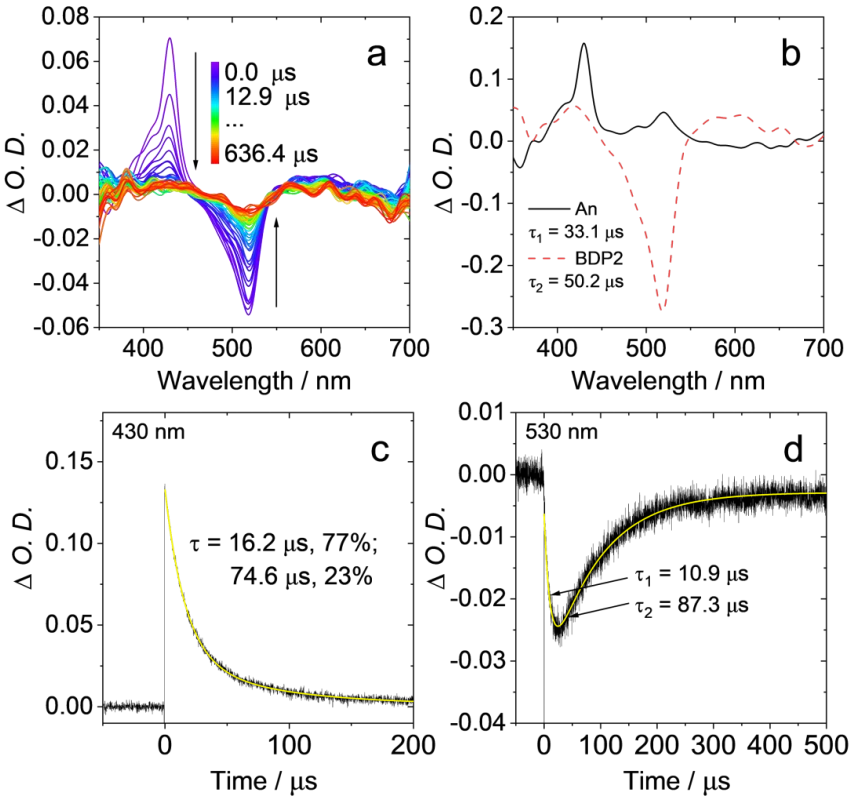

Figure S20. (a) The ns-TA spectra recorded for the mixture of **BDP2** (c = 1.0 × 10^{-5} M) mixing **An** (c = 5.0 × 10^{-6} M) after pulsed laser excitation at 355 nm in deaerated toluene. (b) Evolution associated difference spectra (EADS) based on the data presented in (a). (c) Decay trace of the mixture of **BDP2** and **An** at 430 nm. (d) Decay trace of the mixture of **BDP2** and **An** at 530 nm.

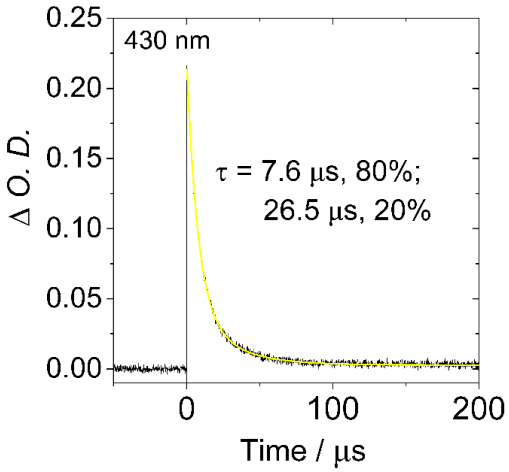

Figure S21. Decay trace of the mixture of **BDP1** and **An** at 430 nm.

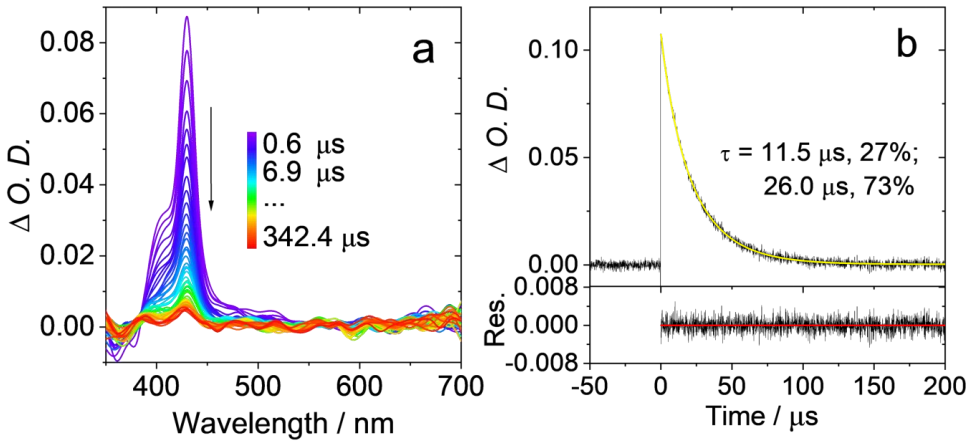

Figure S22. (a) Nanosecond transient absorption spectra of **An** in deaerated toluene. (b) Decay trace at 430 nm. λ_{ex} = 355 nm, c =2.0×10^{-5} M, 20 °C.

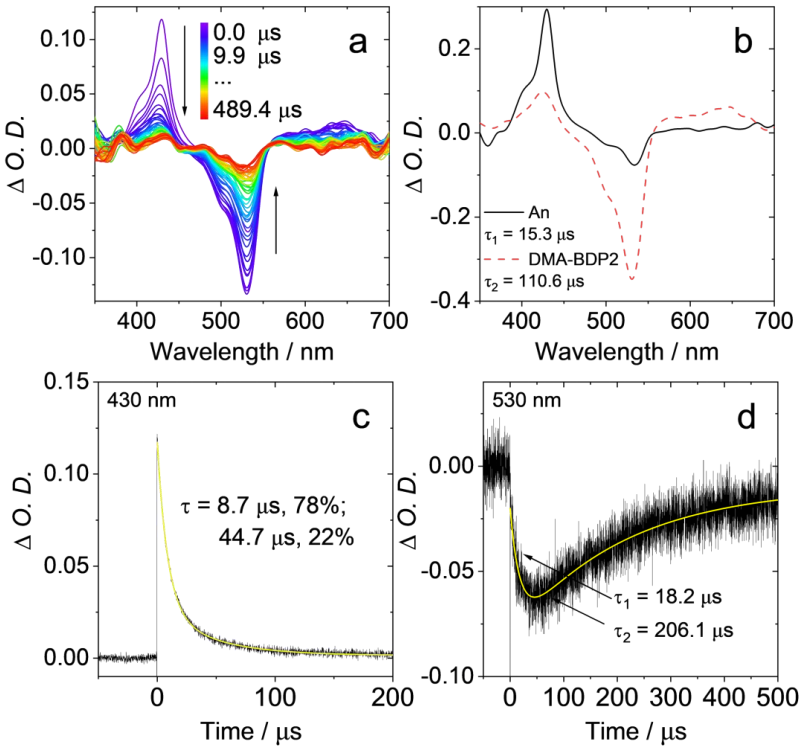

Figure S23. (a) Nanosecond transient absorption (ns-TA) spectra of a deaerated toluene solution containing **DMA-BDP-2** (c = 1.0 × 10^{-5} M) and anthracene (c = 5.0 × 10^{-6} M) recorded after 355 nm pulsed laser excitation. (b) Evolution-associated difference spectra (EADS) obtained from global analysis of the data shown in (a). (c) Kinetic trace at 430 nm, corresponding to the triplet state of anthracene. (d) Kinetic trace at 530 nm, corresponding to the triplet state of **DMA-BDP-2**.

5. Crystallographic Details

Crystals were mounted on a MiTeGen micromount with NVH immersion oil. Data for samples were collected from a shock-cooled single crystal at 100(2) K on either an APEX2 Kappa Duo (Bruker AXS, Karlsruhe, Germany) diffractometer with a microfocus sealed X-ray tube using mirror optics as a monochromator and an APEX2 detector, or on a D8 Quest ECO (Bruker AXS, Karlsruhe, Germany) three-circle diffractometer with a sealed X-ray tube using a graphite as monochromator and a Bruker PHOTON III C7 CMOS Mixed Mode detector. The APEX2 Kappa Duo diffractometer was equipped with a Cobra (Oxford Cryosystems Ltd, Oxford, UK) low temperature device and used Cu K_α radiation (λ = 1.54178 Å), and the D8 Quest ECO with a Cryostream 800 (Oxford Cryosystems Ltd, Oxford, UK) low temperature device and used Mo K_α radiation (λ = 0.71073 Å). All data were integrated with SAINT v8.41B or v8.40B and a multi-scan absorption correction using SADABS 2016/2 was applied.[7a,b,c] The structures were solved by dual methods with SHELXT v2018/2 and refined by full-matrix least-squares methods against F^2 using SHELXL v2019/1.[7d,e] All non-hydrogen atoms were refined with anisotropic displacement parameters. All C-bound hydrogen atoms were refined isotropic on calculated positions using a riding model with their U_{iso} values constrained to 1.5 times the U_{eq} of their pivot atoms for terminal sp^3 carbon atoms and 1.2 times for all other carbon atoms. Disordered moieties were refined using bond lengths restraints and displacement parameter restraints. [7f]

Table S2. Crystal data and refinement details.

Compound	**PA-1**	**DMA-BDP-4**
Identification code	TCD2075	TCD2087
CCDC deposition number	2517531	2517532
Empirical formula	$C_{27}H_{25}NO_4$	$C_{37}H_{39}BF_2N_2O_5$
Formula weight	427.48	640.51
Temperature	100(2) K	100(2) K
Wavelength	1.54178 Å	0.71073 Å
Crystal system	Monoclinic	Monoclinic
Space group	$P2_1/n$	Pc
Unit cell dimensions	a = 9.4818(4) Å a = 90°. b = 12.1507(5) Å b = 102.5809(11)°. c = 18.8527(8) Å g = 90°.	a = 12.0547(6) Å a= 90°. b = 16.3741(8) Å b= 95.033(2)°. c = 8.2479(4) Å g = 90°.
Volume	2119.88(15) $Å^3$	1621.73(14) $Å^3$
Z	4	2
Density (calculated)	1.339 Mg/m^3	1.312 Mg/m^3
Absorption coefficient	0.723 mm^{-1}	0.094 mm^{-1}
F(000)	904	676
Crystal size	0.292 x 0.24 x 0.156 mm^3	0.339 x 0.198 x 0.068 mm^3
Theta range for data collection	4.360 to 68.486°.	2.103 to 27.345°.
Index ranges	-11≤h≤11, -14≤k≤14, -22≤l≤22	-15≤h≤15, -21≤k≤21, -10≤l≤10
Reflections collected	27705	48249
Independent reflections	3900 [R(int) = 0.0325]	7277 [R(int) = 0.0722]
Completeness to theta = 67.6°	99.9 %	99.9 %
Absorption correction	Semi-empirical from equivalents	Semi-empirical from equivalents
Max. and min. transmission	0.7531 and 0.6745	0.7455 and 0.7045

Refinement method	Full-matrix least-squares on F^2	Full-matrix least-squares on F^2
Data / restraints / parameters	3900 / 0 / 295	7277 / 3 / 436
Goodness-of-fit on F^2	1.050	1.085
Final R indices [I>2σ(I)]	R1 = 0.0373, wR2 = 0.0979	R1 = 0.0518, wR2 = 0.1173
R indices (all data)	R1 = 0.0376, wR2 = 0.0983	R1 = 0.0676, wR2 = 0.1260
Largest diff. peak and hole	0.242 and -0.244 e.Å^{-3}	0.325 and -0.307 e.Å^{-3}
Extinction coefficient		0.015(2)
Absolute structure parameter		0.1(4)

Refinement Notes:

TCD2075: Donor N-H hydrogen located and refined semi-free. Model has Chirality at C4, R; C19, S as shown in centrosymmetric space group.

TCD2087: Donor hydrogen atom on the methanol located and refined with geometric restraints (DFIX). The molecule crystallizes in the polar space group, Pc. The chirality at C16, is shown as S; C31, R. The absolute structure determination is unknown (insufficient information) in this all-light atom structure using Mo radiation.

Deposition Numbers 2517531 (for **PA-1**) and 2517532 (for **DMA-BDP-4**) contain the supplementary crystallographic data for this paper. These data are provided free of charge by the joint Cambridge Crystallographic Data Centre and Fachinformationszentrum Karlsruhe Access Structures service www.ccdc.cam.ac.uk/structures.

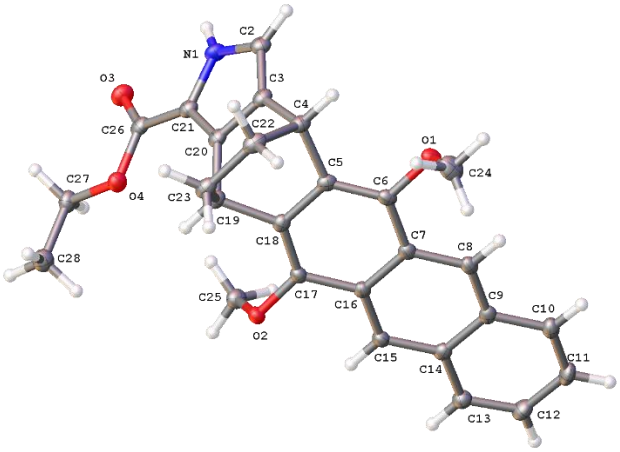

Figure S24. Molecular structure of **PA-1** in the crystal. Atomic displacement shown at 50% probability.

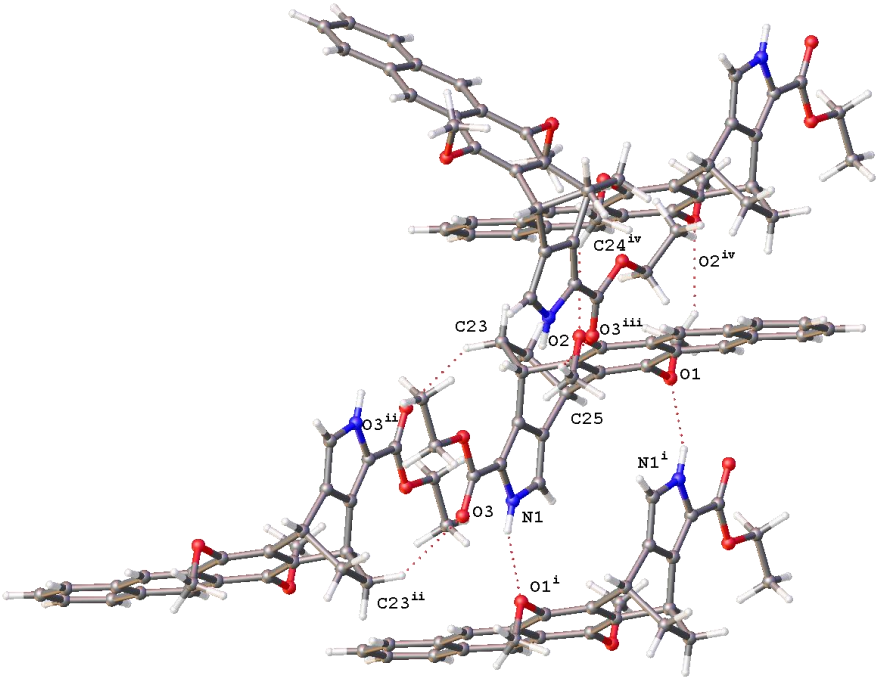

Figure S25. Detail of the potential hydrogen bonding contacts in **PA-1**. Only atoms involved are labelled. Symmetry transformations: i = 1-X, 1-Y, 1-Z; ii = 2-X, 1-Y, 1-Z; iii = 3/2-X, 1/2+Y, 1/2-Z; iv = 1-X, 2-Y, 1-Z

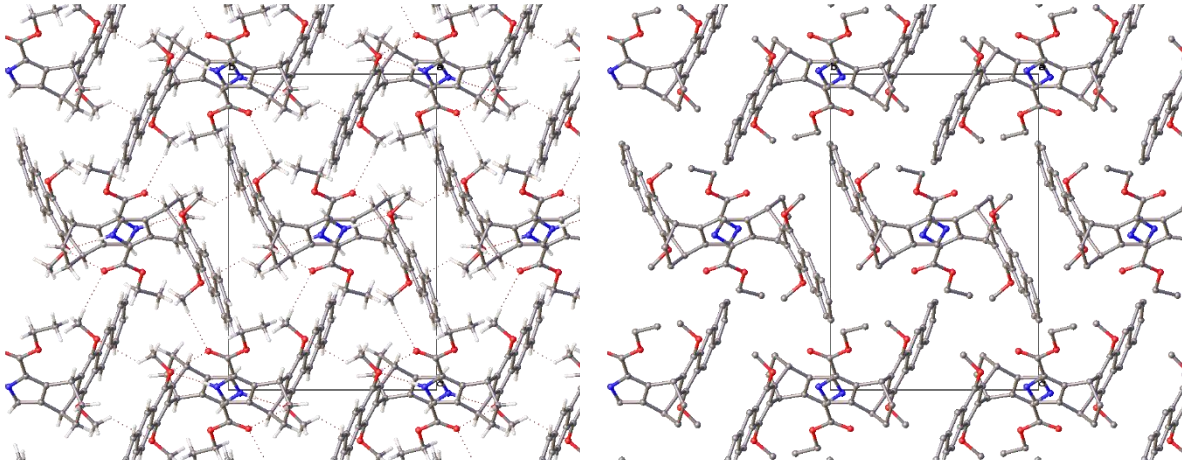

Figure S26. Schematic packing diagram of the majority occupied moiety in **PA-1**, viewed normal to the a-axis, with hydrogen bonds and without.

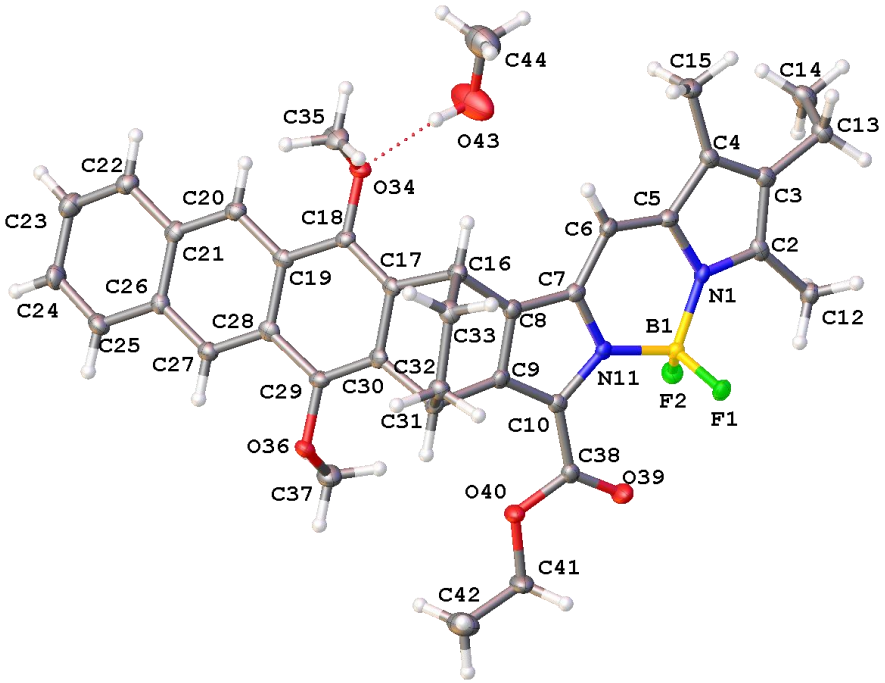

Figure S27. Molecular structure of **DMA-BDP-4** in the crystal with methanol solvate. Atomic displacement shown at 50% probability. Dashed lines indicate hydrogen bonding.

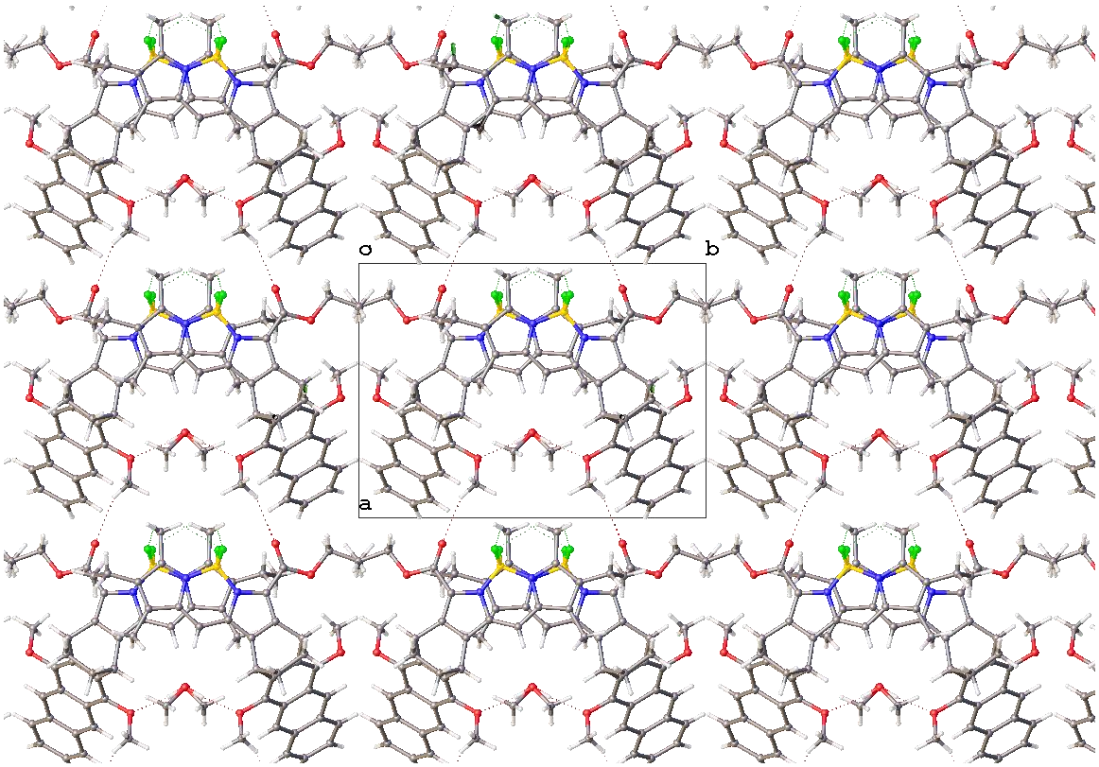

Figure S28. Schematic packing diagram of **DMA-BDP-4** viewed normal to the c-axis. Dotted lines indicate inter and intra molecular hydrogen bonding possibilities.

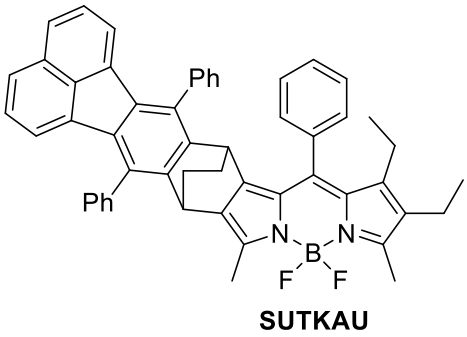

SUTKAU

Figure S29. Structure of the reference compound SUTKAU.[8]

6. Computational Data

The geometries of the compounds were optimized using density functional theory (DFT) at the B3LYP/6-31G(d) level. The spin density surfaces at the optimized triplet state geometries were visualized. The impact of the solvent was included by means of a polarizable continuum model (PCM) to simulate the acetonitrile environment. The triplet excited state energy of the compounds was calculated by time dependent DFT (TDDFT) with the B3LYP functional and 6-31G(d) basis set based on the optimized ground-state geometry. All calculations were performed using Gaussian 16.[9]

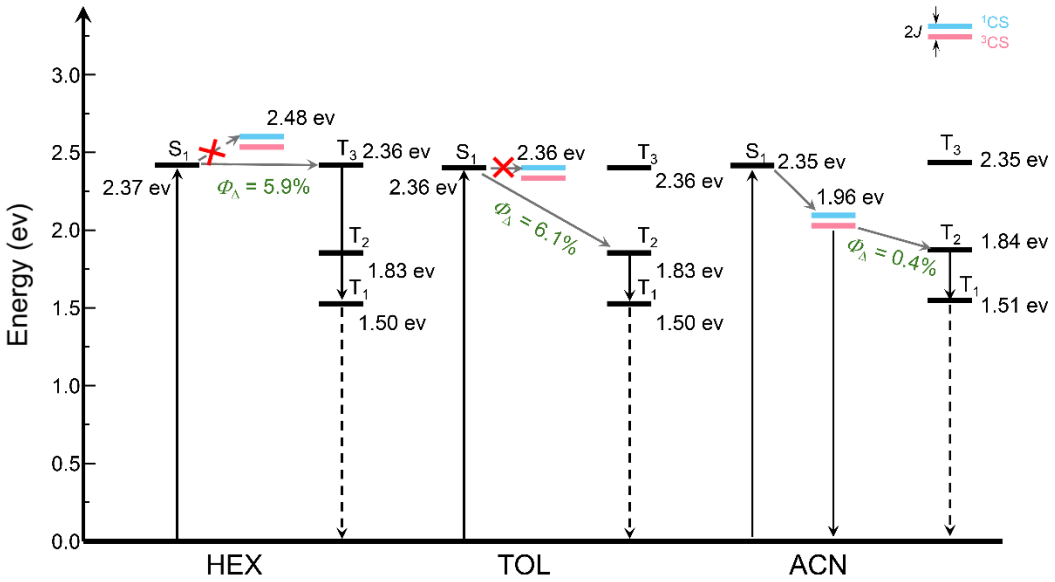

Scheme S1. Photophysical processes of **DMA-BDP-2** in different solvents. The energy of the excited states is calculated by TDDFT at the B3LYP/6-31G(d) level using Gaussian 16; the energy of CT states is obtained by electrochemical calculation.

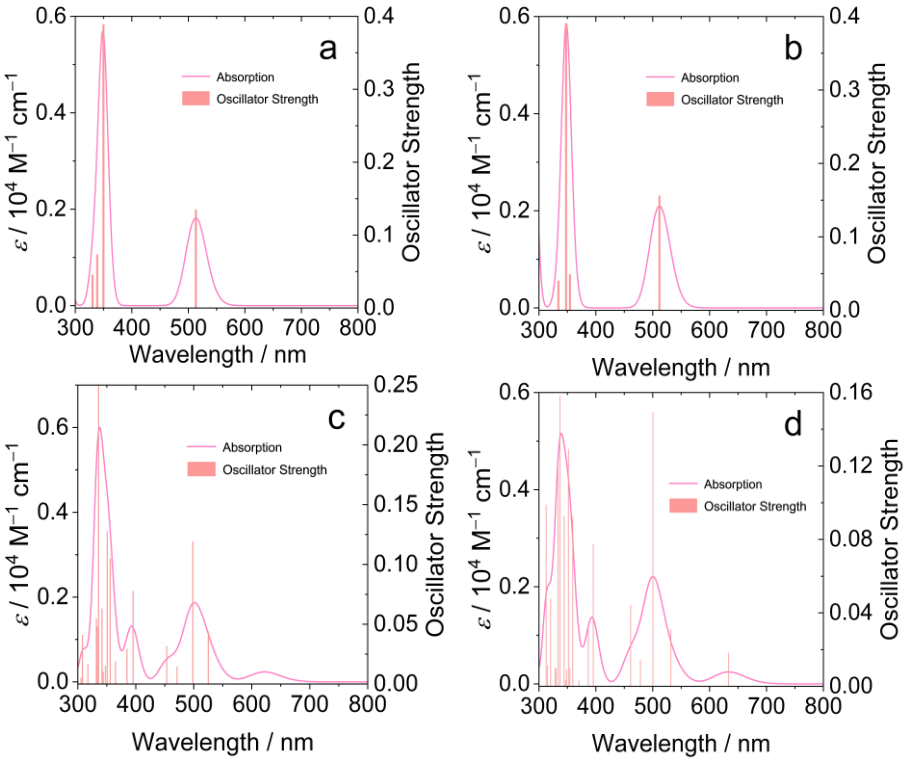

Figure S30. The calculated UV-vis absorption spectra of anions of (a) **BDP-1**, (b) **BDP-2**, (c) **DMA-BDP-1** and (d) **DMA-BDP-2**. These compounds were calculated at the DFT//B3LYP/6-31G(d) level with *Gaussian 16.*

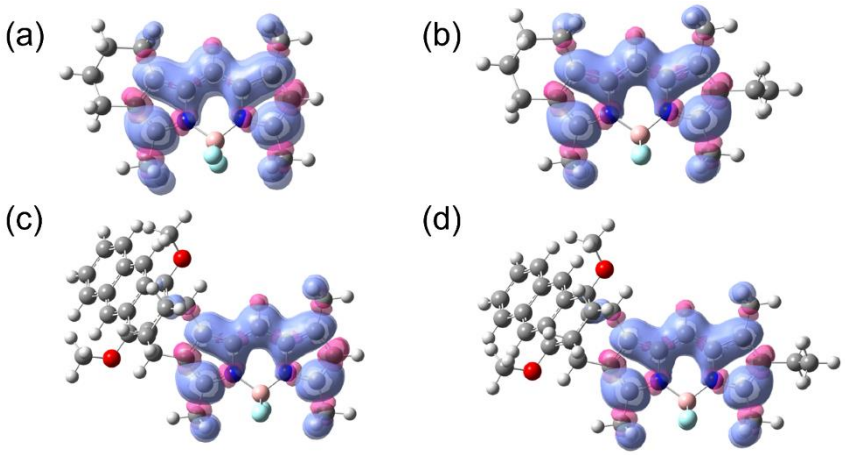

Figure S31. Spin density isosurfaces of (a) **BDP-1**, (b) **BDP-2**, (c) **DMA-BDP-1**, and (d) **DMA-BDP-2**, calculated at the optimized triplet (T_1) geometries using the UB3LYP/6-31G(d) level of theory with Gaussian 16. Solvent effects were included via the CPCM model for acetonitrile. The isovalue was set to 0.0008.

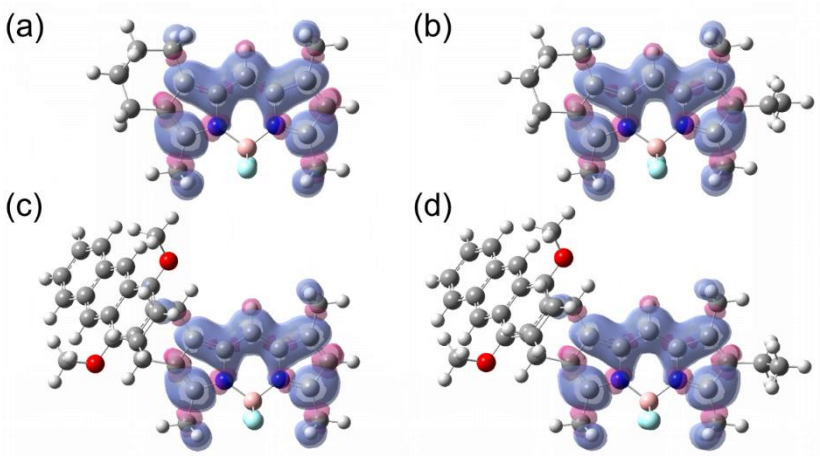

Figure S32. Spin density isosurfaces of (a) **BDP-1**, (b) **BDP-2**, (c) **DMA-BDP-1**, and (d) **DMA-BDP-2**, calculated by DFT at the optimized triplet (T_1) geometries in the gas phase. Calculations were performed using the UB3LYP/6-31G(d) level of theory with Gaussian 16. The isovalue was set to 0.0008.

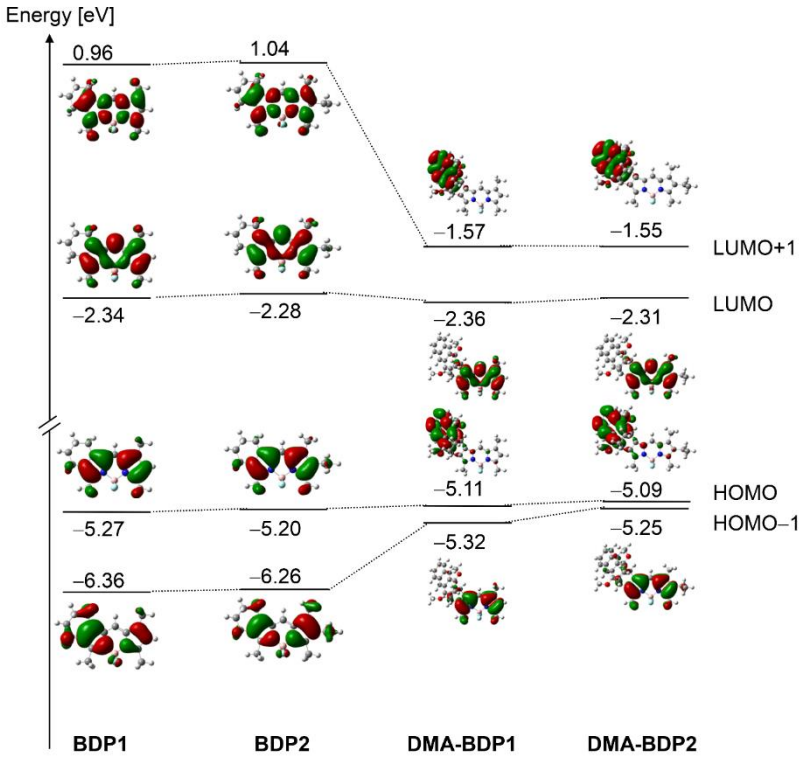

Figure S33. Selected frontier molecular orbitals and corresponding energy levels (in eV) of **BDP-1**, **BDP-2**, **DMA-BDP-1**, and **DMA-BDP-2**, calculated by DFT at the B3LYP/6-31G(d) level using Gaussian 16. Calculations were performed on optimized ground-state geometries. The isovalue for orbital visualization was set to 0.0004.

Coordinates of the Optimized Geometries of the Molecules

BDP1

Symbolic Z-matrix:

Charge = 0 Multiplicity = 1

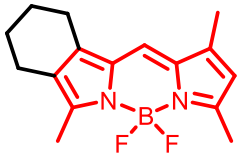

BDP-1

C	−3.45205	−0.23985	−0.067
C	−2.92741	1.9694	0.00245
C	−1.74247	1.17733	0.01989
C	−0.40174	1.54428	0.07063
C	0.62181	0.60491	0.07877
C	2.0356	0.75366	0.12607
C	1.4936	−1.44239	0.05426
N	−2.10621	−0.16986	−0.02397
N	0.33095	−0.7609	0.03547
B	−1.10931	−1.37801	−0.02201
F	−1.32783	−2.17308	1.09872
F	−1.25983	−2.1199	−1.18948
C	−3.98617	1.06992	−0.05163
C	2.57639	−0.52434	0.11065
H	−5.04144	1.31067	−0.07773
C	−4.18477	−1.54032	−0.12056
H	−5.26466	−1.37411	−0.14699
H	−3.88662	−2.1125	−1.00587
H	−3.93624	−2.15685	0.75013
C	−2.99776	3.46663	0.03045
H	−2.47872	3.88355	0.90255
H	−2.54043	3.91244	−0.86223
H	−4.03751	3.80427	0.07155
C	1.54245	−2.93495	0.0194
H	1.00731	−3.35589	0.87772
H	1.04145	−3.31345	−0.87817
H	2.57502	−3.29273	0.03124
C	2.85455	2.00807	0.18279
C	4.04926	−0.80875	0.14859
C	4.85434	0.46796	0.20035
C	4.33314	1.69896	0.21537
H	−0.14679	2.5995	0.10495
H	4.99985	2.55834	0.25852
H	4.43956	1.74517	−0.54121
H	2.63392	2.65793	−0.67923
H	2.58632	2.6096	1.06637
H	4.36078	−1.39926	−0.7279
H	4.30854	−1.43584	1.01689
H	5.93615	0.35069	0.23143
H	5.1996	0.29759	−0.46911

BDP2

Symbolic Z-matrix:

Charge = 0 Multiplicity = 1

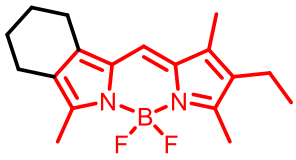

BDP-2

C	3.43804	−0.26906	−0.00119
C	2.93382	1.94593	−0.01529
C	1.74121	1.1662	−0.01237
C	0.40273	1.54706	−0.01652
C	−0.62987	0.61853	−0.01067
C	−2.04349	0.78385	−0.00846
C	−1.52203	−1.4197	0.01327
N	2.09203	−0.1849	−0.0036
N	−0.3517	−0.75075	0.00098
B	1.08287	−1.38257	0.00346
F	1.26151	−2.15904	−1.13843
F	1.25967	−2.14836	1.15131
C	3.98478	1.0351	−0.00876
C	−2.59849	−0.49145	0.00574
C	4.1582	−1.57771	0.00812
H	5.24013	−1.42278	0.00945
H	3.87719	−2.16415	0.88968
H	3.88094	−2.17474	−0.8675
C	3.01906	3.44273	−0.01905
H	2.48736	3.88	−0.87344
H	2.58404	3.87784	0.88992
H	4.06126	3.77061	−0.07508
C	−1.58365	−2.91189	0.04186
H	−0.96022	−3.33529	−0.75197
H	−1.18898	−3.29493	0.99024
H	−2.61175	−3.26241	−0.07925
C	−2.85468	2.04793	−0.03564
C	−4.07909	−0.7581	0.02696
C	−4.85935	0.51394	−0.36091
C	−4.31542	1.75719	0.36242
H	0.1573	2.60505	−0.02224
H	−4.93946	2.63078	0.13993
H	−4.37043	1.59634	1.44805
H	−2.42359	2.80894	0.62824
H	−2.83301	2.48169	−1.0473
H	−4.39134	−1.08426	1.03101
H	−4.34285	−1.5805	−0.65108
H	−4.78343	0.66917	−1.44631
H	−5.92366	0.3791	−0.13499
C	4.75214	1.22426	−1.25857

C	5.79999	1.2145	−2.33221
H	4.75496	2.19888	−0.71257
H	4.93751	0.40891	−0.51774
H	5.79755	0.2401	−2.87838
H	5.61432	2.03004	−3.07281
H	6.81627	1.3661	−1.89373

DMA-BDP-1

Symbolic Z-matrix:

Charge = 0 Multiplicity = 1

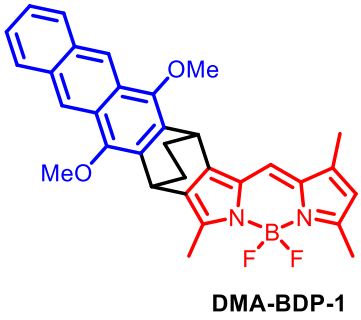

DMA-BDP-1

C	−0.29424	−0.38046	−0.43497
C	1.97812	−0.32321	−0.43613
C	1.51891	−1.68365	−0.43464
C	2.20888	−2.90723	−0.43441
C	1.51884	−4.13078	−0.43441
C	1.97809	−5.4912	−0.4334
C	−0.29429	−5.434	−0.43476
N	0.11898	−1.66212	−0.43408
N	0.11894	−4.15231	−0.43506
B	−0.81701	−2.90721	−0.434
F	−1.61097	−2.90784	0.71138
F	−1.61241	−2.90655	−1.57831
C	0.8338	0.46552	−0.43619
C	0.83374	−6.27994	−0.43375
H	0.80128	1.54773	−0.43724
C	−1.73859	0.00121	−0.43586
H	−1.84781	1.08871	−0.42834
H	−2.24304	−0.40596	−1.31863
H	−2.2475	−0.41894	0.4381
C	3.37963	0.21361	−0.43735
H	3.94583	−0.10437	0.44467
H	3.94988	−0.1182	−1.31152
H	3.35482	1.30784	−0.44578
C	−1.73867	−5.81557	−0.43505
H	−2.24507	−5.40333	0.44421
H	−2.24561	−5.40024	−1.31251
H	−1.84799	−6.90308	−0.4368
H	3.18726	−2.89229	−0.11901
C	1.93735	−7.47972	−1.70211
C	1.04588	−7.53051	−0.46434
C	3.06122	−6.01349	−0.02396
C	3.13558	−6.57686	−1.44046
H	2.28024	−8.51461	−1.95791
H	1.34608	−7.09672	−2.57257

H	4.08855	−7.15181	−1.56402
H	3.15381	−5.73362	−2.17709
H	3.94349	−5.34933	0.16883
H	0.1636	−8.19465	−0.65715
C	6.56776	−12.16277	4.64547
C	6.47625	−10.89101	4.1592
C	5.37627	−10.50172	3.32762
C	4.37639	−11.4718	3.01047
C	4.50852	−12.79703	3.539
C	5.5689	−13.13029	4.33065
C	5.26039	−9.20214	2.82251
C	3.29659	−11.1085	2.19837
C	3.18034	−9.80868	1.69383
C	4.1792	−8.83812	2.01252
C	4.04395	−7.51139	1.48866
C	2.98124	−7.17699	0.70058
C	1.98488	−8.14575	0.38195
C	2.08033	−9.41951	0.86231
H	6.03092	−8.45476	3.06706
H	7.40954	−12.46444	5.28608
H	7.24022	−10.13492	4.39516
H	3.73196	−13.53492	3.28705
H	5.67424	−14.14663	4.738
H	2.52629	−11.85621	1.95413
O	4.68431	−6.66297	1.7008
O	1.43976	−10.12281	0.63229
C	5.59325	−5.6146	1.77273
H	6.4333	−6.26715	1.65698
H	5.61901	−5.16911	2.74524
H	5.63225	−4.84744	1.02785
C	0.97976	−11.26145	0.35117
H	0.30757	−11.36417	−0.47496
H	0.43096	−11.32475	1.26753
H	1.70877	−12.04395	0.31725

DMA-BDP-2

Symbolic Z-matrix:

Charge = 0 Multiplicity = 1

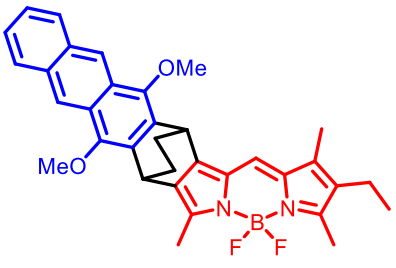

DMA-BDP-2

C	−0.29424	−0.38046	−0.43497
C	1.97812	−0.32321	−0.43613
C	1.51891	−1.68365	−0.43464
C	2.20888	−2.90723	−0.43441
C	1.51884	−4.13078	−0.43441

C	1.97809	−5.4912	−0.4334
C	−0.29429	−5.434	−0.43476
N	0.11898	−1.66212	−0.43408
N	0.11894	−4.15231	−0.43506
B	−0.81701	−2.90721	−0.434
F	−1.61097	−2.90784	0.71138
F	−1.61241	−2.90655	−1.57831
C	0.8338	0.46552	−0.43619
C	0.83374	−6.27994	−0.43375
C	−1.73859	0.00121	−0.43586
H	−1.84781	1.08871	−0.42834
H	−2.24304	−0.40596	−1.31863
H	−2.2475	−0.41894	0.4381
C	3.37963	0.21361	−0.43735
H	3.94583	−0.10437	0.44467
H	3.94988	−0.1182	−1.31152
H	3.35482	1.30784	−0.44578
C	−1.73867	−5.81557	−0.43505
H	−2.24507	−5.40333	0.44421
H	−2.24561	−5.40024	−1.31251
H	−1.84799	−6.90308	−0.4368
H	3.18726	−2.89229	−0.11901
C	1.93735	−7.47972	−1.70211
C	1.04588	−7.53051	−0.46434
C	3.06122	−6.01349	−0.02396
C	3.13558	−6.57686	−1.44046
H	2.28024	−8.51461	−1.95791
H	1.34608	−7.09672	−2.57257
H	4.08855	−7.15181	−1.56402
H	3.15381	−5.73362	−2.17709
H	3.94349	−5.34933	0.16883
H	0.1636	−8.19465	−0.65715
C	6.56776	−12.16277	4.64547
C	6.47625	−10.89101	4.1592
C	5.37627	−10.50172	3.32762
C	4.37639	−11.4718	3.01047
C	4.50852	−12.79703	3.539
C	5.5689	−13.13029	4.33065
C	5.26039	−9.20214	2.82251
C	3.29659	−11.1085	2.19837
C	3.18034	−9.80868	1.69383
C	4.1792	−8.83812	2.01252
C	4.04395	−7.51139	1.48866
C	2.98124	−7.17699	0.70058
C	1.98488	−8.14575	0.38195

C	2.08033	−9.41951	0.86231
H	6.03092	−8.45476	3.06706
H	7.40954	−12.46444	5.28608
H	7.24022	−10.13492	4.39516
H	3.73196	−13.53492	3.28705
H	5.67424	−14.14663	4.738
H	2.52629	−11.85621	1.95413
O	4.68431	−6.66297	1.7008
O	1.43976	−10.12281	0.63229
C	5.59325	−5.6146	1.77273
H	6.4333	−6.26715	1.65698
H	5.61901	−5.16911	2.74524
H	5.63225	−4.84744	1.02785
C	0.97976	−11.26145	0.35117
H	0.30757	−11.36417	−0.47496
H	0.43096	−11.32475	1.26753
H	1.70877	−12.04395	0.31725
C	1.71735	2.81359	−0.94047
C	1.10425	1.7372	−0.09415
H	2.82728	2.83079	−0.81494
H	1.49119	2.64369	−2.02121
H	1.31838	3.81702	−0.65419
H	1.50353	0.73393	−0.38068
H	1.33079	1.90725	0.98651

DMA-BDP-4

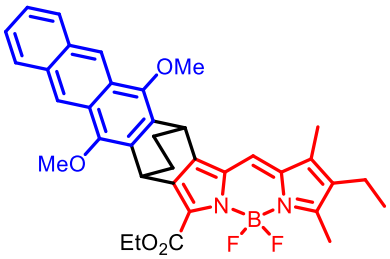

DMA-BDP-4

Symbolic Z-matrix:
Charge = 0 Multiplicity = 1

B	-3.65985	0.93652	-0.02568
F	-4.45861	1.69594	0.80366
N	-4.25554	-0.53945	-0.03893
C	-5.45649	-0.89694	-0.50679
F	-3.62575	1.39354	-1.32764
C	-5.67163	-2.30179	-0.28906
C	-4.53786	-2.78898	0.34375
C	-3.64804	-1.67323	0.50047
C	-2.3901	-1.58115	1.04608
H	-1.91848	-2.46713	1.45984
C	-1.66521	-0.37529	1.06448
C	-0.3459	-0.12864	1.49251
C	-0.06345	1.20656	1.22083
C	-1.22135	1.76818	0.6483

N	-2.19298	0.80558	0.55544
C	-6.37962	0.08909	-1.14278
H	-5.94142	0.47491	-2.06969
H	-6.51743	0.95106	-0.48227
H	-7.35045	-0.35919	-1.36429
C	-6.89247	-3.0711	-0.71239
H	-7.78993	-2.45958	-0.55421
H	-7.01065	-3.94832	-0.06456
C	-6.84972	-3.53378	-2.1814
H	-7.75752	-4.09035	-2.44066
H	-5.98729	-4.18451	-2.36297
H	-6.76945	-2.68039	-2.8638
C	-4.24516	-4.19561	0.76849
H	-3.7219	-4.75412	-0.01917
H	-5.16606	-4.74237	0.99482
H	-3.61362	-4.22582	1.66278
C	0.76541	-0.88963	2.16234
H	0.54631	-1.94441	2.33822
C	2.00406	-0.70381	1.29647
C	2.82004	-1.7163	0.81892
C	3.94434	-1.41188	0.00786
C	4.77918	-2.4495	-0.53286
H	4.53139	-3.48274	-0.31217
C	5.41129	0.28535	-1.05184
H	5.62103	1.33033	-1.25528
C	4.25481	-0.03897	-0.26247
C	3.39907	0.97824	0.23831
C	2.29142	0.65109	1.00471
C	1.31963	1.63469	1.64671
H	1.56093	2.66863	1.41159
O	2.51691	-3.0398	1.08901
C	3.13654	-3.55638	2.26911
H	2.80038	-3.0181	3.16528
H	4.23022	-3.4925	2.20688
H	2.83642	-4.60447	2.34193
O	3.71299	2.29848	-0.01637
C	3.05761	2.84924	-1.16621
H	1.9703	2.87258	-1.0313
H	3.30103	2.27577	-2.06975
H	3.43491	3.86944	-1.27077
C	-1.44668	3.16923	0.23201
O	-2.52062	3.69084	0.0318
O	-0.2579	3.82992	0.1255
C	1.05431	-0.12046	3.5015
H	0.17376	-0.19204	4.14811
H	1.88427	-0.61062	4.02215
C	1.39806	1.36791	3.19197

H	2.40597	1.61455	3.54113
H	0.70047	2.04038	3.70122
C	-0.34742	5.23522	-0.21382
H	0.58155	5.66306	0.17174
H	-1.19611	5.67022	0.3196
C	-0.47975	5.44489	-1.71501
H	-0.47936	6.51796	-1.93943
H	0.35607	4.98285	-2.25121
H	-1.41608	5.01638	-2.08141
C	6.18734	-0.71885	-1.55925
C	5.87879	-2.11575	-1.27292
C	7.38022	-0.28694	-2.43222
H	7.53725	0.72826	-2.73155
C	8.27411	-1.25016	-2.91916
H	8.9735	-0.81829	-3.60418
C	8.03471	-3.0353	-2.26928
H	8.58834	-3.94309	-2.14958
C	6.74853	-3.28464	-1.77178
H	6.38838	-4.29215	-1.76081

Table S3. Comparison of DFT-optimized and experimentally obtained structural parameters of **BDP-DMA-4**.

Parameter	DFT-Optimized	Crystal
Alpha C–N (pyrrolic A)	1.370174 Å	1.38598(7) Å
Alpha C–N (pyrrolic B)	1.338267 Å	1.33235(5) Å
B–N (pyrrolic A)	1.582224 Å	1.56210(6) Å
B–N (pyrrolic B)	1.591421 Å	1.57793(7) Å
Alpha C–carbonyl C	1.478921 Å	1.45804(5) Å
a-angle	106.292693°	106.420(2)°
b-angle	105.758642°	106.3127(15)°
RMSD	0.055 Å	0.051 Å

Table S4. Spin-orbit coupling matrix elements (SOCME) (cm^{-1} units) for the State Pairs Evaluated at the Optimized Geometry of the Ground State.[a]

Compounds	ISC	SOCME	ΔE [b]
BDP-1	$S_1 \rightarrow T_1$	0.09	1.467
	$S_1 \rightarrow T_2$	0.19	0.274
	$S_1 \rightarrow T_3$	1.70	0.005
	$T_1 \rightarrow S_0$	0.24	1.418
BDP-2	$S_1 \rightarrow T_1$	0.02	1.414
	$S_1 \rightarrow T_2$	0.07	0.260
	$S_1 \rightarrow T_3$	1.80	0.055
	$T_1 \rightarrow S_0$	0.19	1.417
DMA-BDP-1	$S_2 \rightarrow T_1$	0.18	1.404
	$S_2 \rightarrow T_2$	0.05	1.05
	$S_2 \rightarrow T_3$	0.17	0.588
	$S_2 \rightarrow T_4$	0.13	0.307
	$S_2 \rightarrow T_5$	1.96	0.004
	$T_1 \rightarrow S_0$	0.22	1.459
DMA-BDP-2	$S_2 \rightarrow T_1$	0.15	1.533
	$S_2 \rightarrow T_2$	0.07	0.946
	$S_2 \rightarrow T_3$	0.21	0.510
	$S_2 \rightarrow T_4$	0.13	0.257
	$S_2 \rightarrow T_5$	1.23	0.079
	$T_1 \rightarrow S_0$	0.27	1.224
DMA-BDP-3	$S_3 \rightarrow T_1$	0.72	1.509
	$S_3 \rightarrow T_2$	0.16	1.195
	$S_3 \rightarrow T_3$	0.43	1.033
	$S_3 \rightarrow T_4$	0.52	0.569
	$S_3 \rightarrow T_5$	1.97	0.306
	$T_1 \rightarrow S_0$	0.75	1.472
DMA-BDP-4	$S_2 \rightarrow T_1$	0.30	1.295
	$S_2 \rightarrow T_2$	0.09	0.968
	$S_2 \rightarrow T_3$	0.24	0.766
	$S_2 \rightarrow T_4$	0.63	0.370
	$S_2 \rightarrow T_5$	2.30	0.186
	$T_1 \rightarrow S_0$	0.66	1.466

[a] The calculation of the spin orbital coupling matrix elements (SOCMEs) were performed at B3LYP/def2-SVP level using the ORCA 6.1.0 programs.[10]

7. References

[1] R. F. Kubin, A. N. Fletcher *J. Lumin.,* **1982**, *27*, 455–462.
[2] M. A. Filatov, F. Etzold, D. Gehrig, F. Laquai, D. Busko, K. Landfester, S. Baluschev, *Dalton Trans.* **2015**, *44*, 19207–19217.
[3] T. Mikulchyk, S. Karuthedath, C. S. P. De Castro, A. A. Buglak, A. Sheehan, A. Wieder, F. Laquai, I. Naydenova, M. A. Filatov, *J. Mater. Chem. C* **2022**, *10*, 11588–11597.
[4] S. Ito, M. Akaki, Y. Shinozaki, Y. Iwabe, M. Furuya, M. Tobata, M. Roppongi, T. Sato, N. Itoh, T. Oba, *Tetrahedron Lett.* **2017**, *58*, 1338–1342.
[5] B. R. Groves, T. S. Cameron, A. Thompson, *Org. Biomol. Chem.* **2017**, *15*, 7925.
[6] (a) R. Ziessel, B. Allen, D. Rewinska and A. Harriman, *Chem. Eur. J., **2009**, 15, 7382–7393.*; (b) D. I. Schuster, P. Cheng, P. D. Jarowski, D. M. Guldi, C. Luo, L. Echegoyen, S. Pyo, A. R. Holzwarth, S. E. Braslavsky, R. M. Williams and G. Klihm, *J. Am. Chem. Soc.*, **2004**, *126*, 7257–7270; (c) S. Shao, H. B. Gobeze, V. Bandi, C. Funk, B. Heine, M. J. Duffy, V. Nesterov, P. A. Karr and F. D'Souza, *ChemPhotoChem, **2020**, 4,* 68; (d) W.-J. Shi, M. E. El-Khouly, K. Ohkubo, S. Fukuzumi and D. K. P. Ng, *Chem. Eur. J.*, **2013**, *19*, 11332–11341.
[7] (a) Bruker, APEX3 V2017.3-0, Bruker AXS Inc., Madison, Wisconsin, (USA), 2017; (b) Bruker, *SAINT*, *v8.37A*, Bruker AXS Inc., Madison, Wisconsin, USA; (c) L. Krause, R. Herbst-Irmer, G. M. Sheldrick and D. Stalke, *J. Appl. Crystallogr.* **2015**, *48*, 3–10; (d) G. M. Sheldrick, *Acta Crystallogr.* **2015**, *A71*, 3–8; (e) G. M. Sheldrick, *Acta Crystallogr.* **2015**, *C71*, 3–8; (f) O. V. Dolomanov, L. J. Bourhis, R. J. Gildea, J. A. K. Howard and H. Puschmann, *J. Appl. Crystallogr.* **2009**, *42*, 339–341.
[8] T. Okujima, Y. Tomimori, J. Nakamura, H. Yamada, H. Uno, N. Ono, *Tetrahedron,* **2010**, *66*, 6895.
[9] *Gaussian 16, Revision B.01*, M. J. Frisch, G. W. Trucks, H. B. Schlegel, G. E. Scuseria, M. A. Robb, J. R. Cheeseman, G. Scalmani, V. Barone, G. A. Petersson, H. Nakatsuji, X. Li, M. Caricato, A. V. Marenich, J. Bloino, B. G. Janesko, R. Gomperts, B. Mennucci, H. P. Hratchian, J. V. Ortiz, A. F. Izmaylov, J. L. Sonnenberg, D. Williams-Young, F. Ding, F. Lipparini, F. Egidi, J. Goings, B. Peng, A. Petrone, T. Henderson, D. Ranasinghe, V. G. Zakrzewski, J. Gao, N. Rega, G. Zheng, W. Liang, M. Hada, M. Ehara, K. Toyota, R. Fukuda, J. Hasegawa, M. Ishida, T. Nakajima, Y. Honda, O. Kitao, H. Nakai, T. Vreven, K. Throssell, J. A. Montgomery, Jr., J. E. Peralta, F. Ogliaro, M. J. Bearpark, J. J. Heyd, E. N. Brothers, K. N. Kudin, V. N. Staroverov, T. A. Keith, R. Kobayashi, J. Normand, K. Raghavachari, A. P. Rendell, J. C. Burant, S. S. Iyengar, J. Tomasi, M. Cossi, J. M. Millam, M. Klene, C. Adamo, R. Cammi, J. W. Ochterski, R. L. Martin, K. Morokuma, O. Farkas, J. B. Foresman, and D. J. Fox, Gaussian, Inc., Wallingford CT, 2016.
[10] WIRES, *Comput. Molec. Sci.,* **2025,** *15*, e70019